Beyond the Classical Performance Limitations Controlling Uncertain MIMO Systems: UAV Applications

1st Session

Mario Garcia-Sanz

Automatic Control & Computer Science Department
Public University of Navarra
31006 Pamplona, Spain
(Email: mgsanz@unavarra.es)

NATO. RTO-LS-SCI-195, May-June 2008

Report Documentation Page

Form Approved
OMB No. 0704-0188

1. REPORT DATE **MAY 2008**	2. REPORT TYPE	3. DATES COVERED **00-00-2008 to 00-00-2008**
4. TITLE AND SUBTITLE **Beyond the Classical Performance Limitations Controlling Uncertain MIMO Systems: UAV Applications**		5a. CONTRACT NUMBER 5b. GRANT NUMBER 5c. PROGRAM ELEMENT NUMBER
6. AUTHOR(S)		5d. PROJECT NUMBER 5e. TASK NUMBER 5f. WORK UNIT NUMBER
7. PERFORMING ORGANIZATION NAME(S) AND ADDRESS(ES) **Public University of Navarra,Automatic Control & Computer Science Department,31006 Pamplona Spain,**		8. PERFORMING ORGANIZATION REPORT NUMBER
9. SPONSORING/MONITORING AGENCY NAME(S) AND ADDRESS(ES)		10. SPONSOR/MONITOR’S ACRONYM(S) 11. SPONSOR/MONITOR’S REPORT NUMBER(S)

12. DISTRIBUTION/AVAILABILITY STATEMENT
Approved for public release; distribution unlimited

13. SUPPLEMENTARY NOTES
See also ADM002223. Presented at the NATO/RTO Systems Concepts and Integration Panel Lecture Series SCI-195 on Advanced Autonomous Formation Control and Trajectory Management Techniques for Multiple Micro UAV Applications held in Glasgow, United Kingdom on 19-21 May 2008.

14. ABSTRACT

15. SUBJECT TERMS

16. SECURITY CLASSIFICATION OF:			17. LIMITATION OF ABSTRACT	18. NUMBER OF PAGES	19a. NAME OF RESPONSIBLE PERSON
a. REPORT **unclassified**	b. ABSTRACT **unclassified**	c. THIS PAGE **unclassified**	**Same as Report (SAR)**	**76**	

Standard Form 298 (Rev. 8-98)
Prescribed by ANSI Std Z39-18

Outline

1.- QFT Controller Design Technique Fundamentals

2.- Real-world QFT control applications and examples

3.- Non-diagonal MIMO QFT controller design methodologies

4.- Application: Robust QFT control for a MIMO Spacecraft with flexible sunshield

5.- Switching robust control: Beyond the linear limitations.

6.- Example: Switching control for Unmanned Vehicles

1.- QFT Controller Design Technique Fundamentals

1.1.- Introduction

a reliable control design methodology

- Quantitative Feedback Theory (Q.F.T.). Introduced by Prof. Isaac Horowitz.
  - ➔ 1959. First ideas.
  - ➔ 1972. The name.
  - ➔ 1973. Horowitz at the Air Force Office of Scientific Research (first grant).
  - ➔ 1992. Prof. Houpis organizes the First International Symposium on QFT.
  - ➔ Until then, Int. Symposia every two years: 1995, 1997, 1999, 2001, 2003, 2005, 2007.
- The **QFT** design objective is to design and implement a robust control for a system with Uncertainty that satisfies the desired Performance Specifications.
- Frequency Domain Technique. Uses the Nichols Chart (NC).
- Looks for a design that combines:
  - ➔ Model + Parameter Uncertainty. *(Robustness).*
  - ➔ Performance Specifications.
  - ➔ Minimum Order Controller. Transparency of the Technique.
- Achieves reasonably low loop gains, i.e., avoids or minimizes: Sensor noise amplification, Saturation, High Frequency uncertainties.

Mario Garcia-Sanz

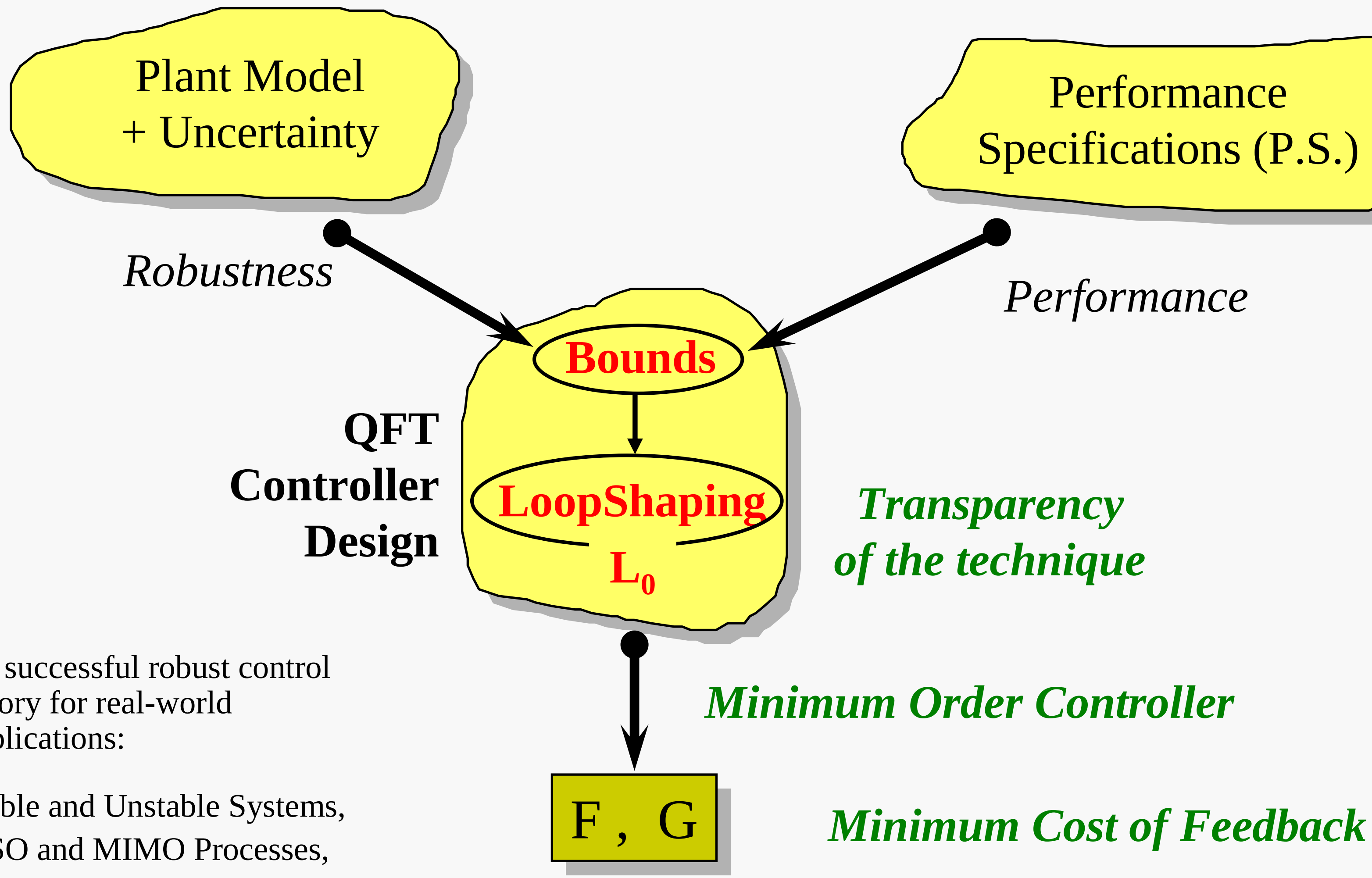

QFT. A successful robust control theory for real-world applications:

- Stable and Unstable Systems,
- SISO and MIMO Processes,
- Analog and Discrete Systems,
- Linear and Non-linear Plants,
- Processes with constant and variable parameters,
- Minimum and Non-minimum Phase Systems,
- Cascade Control Systems, etc.

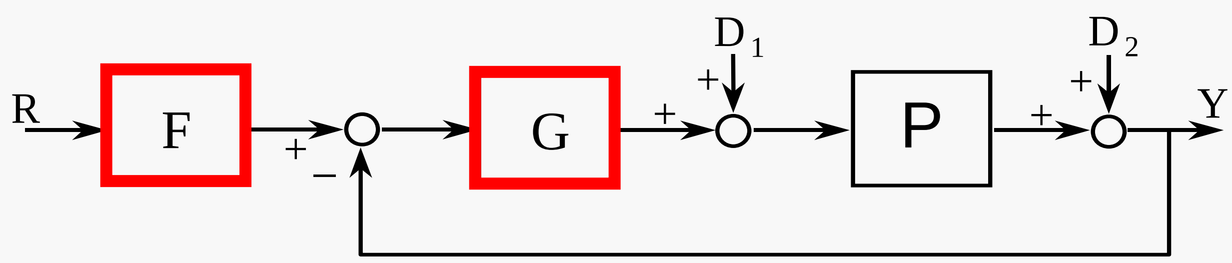

Mario Garcia-Sanz

1.2.- MISO analog control system design

QFT Design Procedure

Control Specifications
- **Step 1**: Control Specifications: Stability
- **Step 2**: Control Specifications: Performance

Model + uncertainty
- **Step 3**: Specify Plant models + Uncertainty
- **Step 4**: Obtain templates at specified ω_i (describes uncertainty)
- **Step 5**: Select nominal plant $P_o(s)$

Bounds
- **Step 6**: Determine stability contour (U-contour) on N.C.
- **Steps 7-9**: Determine tracking, disturbance, & optimal bounds

Loopshaping
- **Step 10**: Synthesize nominal $L_o(s) = G(s)P_o(s)$

  -- Satisfies all bounds & stability contour

  -- Obtain $G(s) = L_o(s)/P_o(s)$

Prefilter
- **Step 11**: Synthesize prefilter F(s).
- **Step 12**: Simulate linear system (J time responses)
- **Step 13**: Simulate with nonlinearities

Step 1, 2: Control Specifications: Stability and Performance

R Reference
W Controller Input Disturbance
V Plant Input Disturbance
D Plant Output Disturbance
N Noise

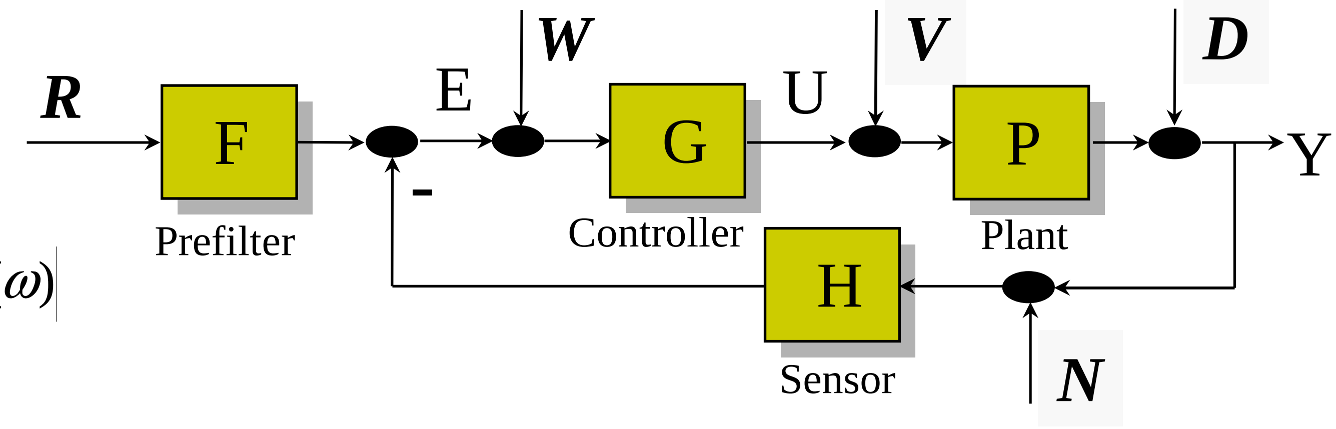

Specifications
in terms of T.F.
For example:

$$\left|\frac{1}{1+PGH}\right| \le \left|W_{S_1}(\omega)\right|$$

$$Y=\frac{1}{1+PGH}D+\frac{P}{1+PGH}V+\frac{PG}{1+PGH}(W+FR)-\frac{PGH}{1+PGH}N \quad (1)$$

$$E=-\frac{H}{1+PGH}D+\frac{PH}{1+PGH}V+\frac{PGH}{1+PGH}W+\frac{1}{1+PGH}FR-\frac{H}{1+PGH}N \quad (2)$$

$$U=\frac{G}{1+PGH}(W+FR)-\frac{GH}{1+PGH}(N+D+PV) \quad (3)$$

Mario Garcia-Sanz

Stability

$$\left|\frac{PGH}{1+PGH}\right| \le W_{s1}$$

The Stability (Gain and Phase Margins) is **related** with the Maximum closed-loop Resonance M_m specification.

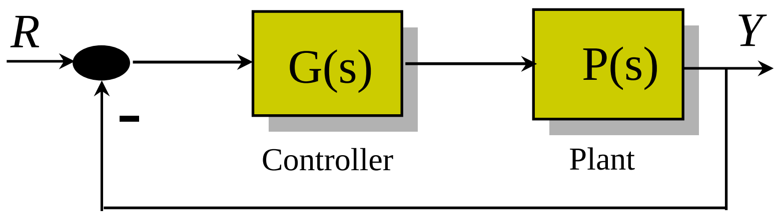

$$\frac{Y(j\omega)}{R(j\omega)} = T(j\omega) = \frac{P(j\omega)\,G(j\omega)}{1+P(j\omega)\,G(j\omega)}$$

$$|T(j\omega)| \le \mu = W_{s1}$$

$$L(j\omega) = P(j\omega)\,G(j\omega) = M\,e^{j\psi}$$

$$GM = 1/M \quad \text{at point} \quad \psi = -180^o$$

$$PM = 180^o + \psi \quad \text{at point} \quad |L(j\omega)| = 1$$

Gain Margin: $GM \ge 1 + 1/\mu$ (magnitude)

Phase Margin: $PM \ge 180^o - \theta$ (deg)

where: μ is the circle M specification in magnitude: $M_m = 20 \log_{10}(\mu)$

$\theta = 2 \cos^{-1}(0.5/\mu) \in [0, 180^o]$

Ws1	GM	PM	Overshoot
1.1 (0.8 dB)	1.99 (5.9 dB)	55º	~ 11 %
1.2 (1.58 dB)	1.83 (5.2 dB)	49º	~ 18 %
1.3 (2.28 dB)	1.77 (5.0 dB)	45º	~ 22 %
1.4 (2.9 dB)	1.71 (4.7 dB)	41.8º	~ 27 %

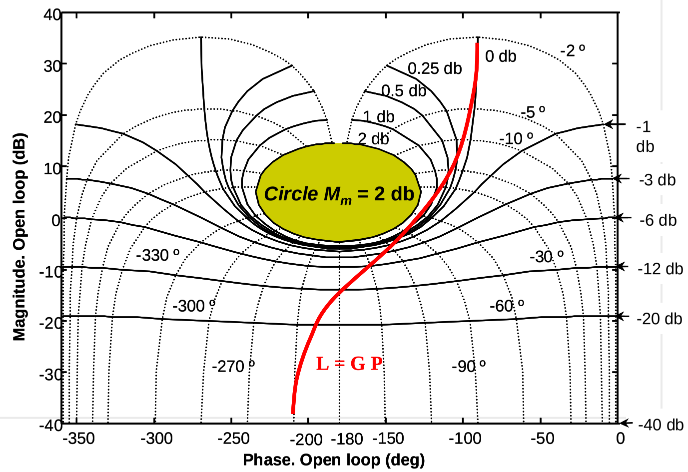

Mario Garcia-Sanz

Performance

Tracking

$$W_{s7a} \le \left| \frac{PG}{1+PGH} \right| \le W_{s7b}$$

- **Time-Domain Specifications:** Desire system output y(t) to lie between specified upper and lower bounds, $y(t)_U$ and $y(t)_L$, respectively.

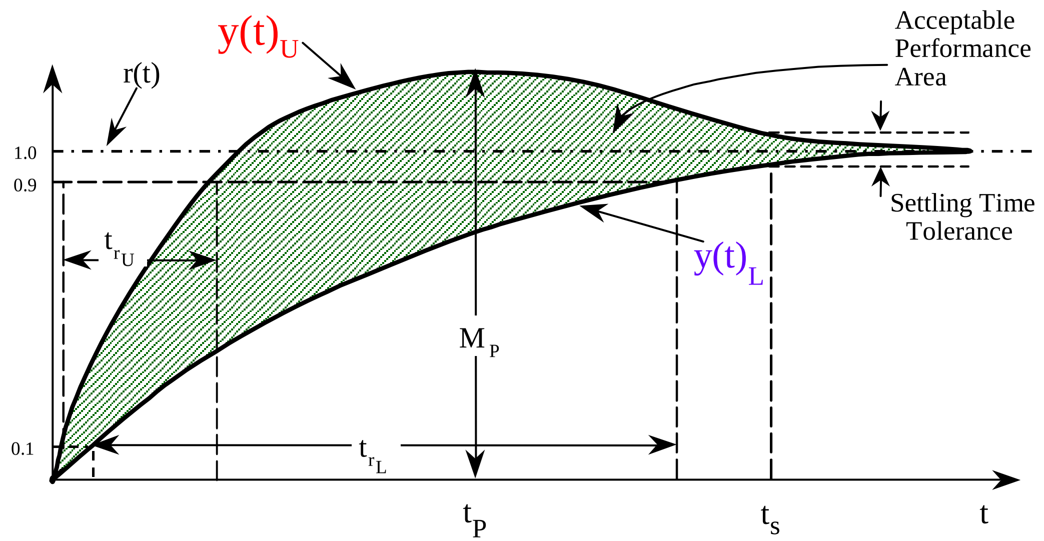

Desired system performance specifications: time domain response specifications;

Figures of merit (FOM), based upon a *step input signal* $r(t) = R_0\, u_{-1}(t)$,

➔ M_p peak overshoot; t_r rise time; t_p peak time; and t_s settling time.

Depends on *requirements* that the designer wants for the *specific Plant*:

➔ Airplane, Heating system, Machinery, Wind Turbine, etc...

Tracking

$$W_{s7a} \le \left| \frac{PG}{1+PGH} \right| \le W_{s7b}$$

<u>Translated into</u> the frequency domain are, $\mathbf{B_U}$ and $\mathbf{B_L}$, the upper and lower bounds respectively: Peak overshoot Lm M_m & frequency bandwidth ω_h .

(Note: increasing $\boldsymbol{\delta_R(j\omega_i)}$ above 0 dB crossing)

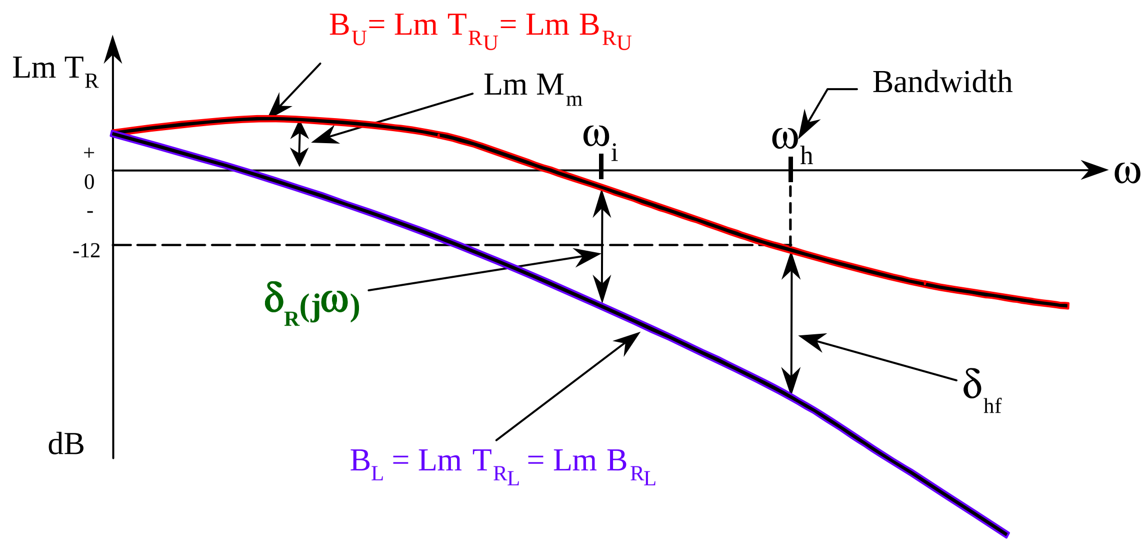

Desired system performance specifications:
frequency domain response specifications.

Mario Garcia-Sanz

Tracking

$$W_{s7a} \le \left| \frac{PG}{1+PGH} \right| \le W_{s7b}$$

Upper function $\quad W_{s7b} = T_{RU} = \dfrac{(\omega_n^{\,2}/a)(s+a)}{s^2 + 2\xi\omega_n s + \omega_n^{\,2}}$

Lower function $\quad W_{s7a} = T_{RL} = \dfrac{k}{(s+\sigma_1)(s+\sigma_2)(s+\sigma_3)}$

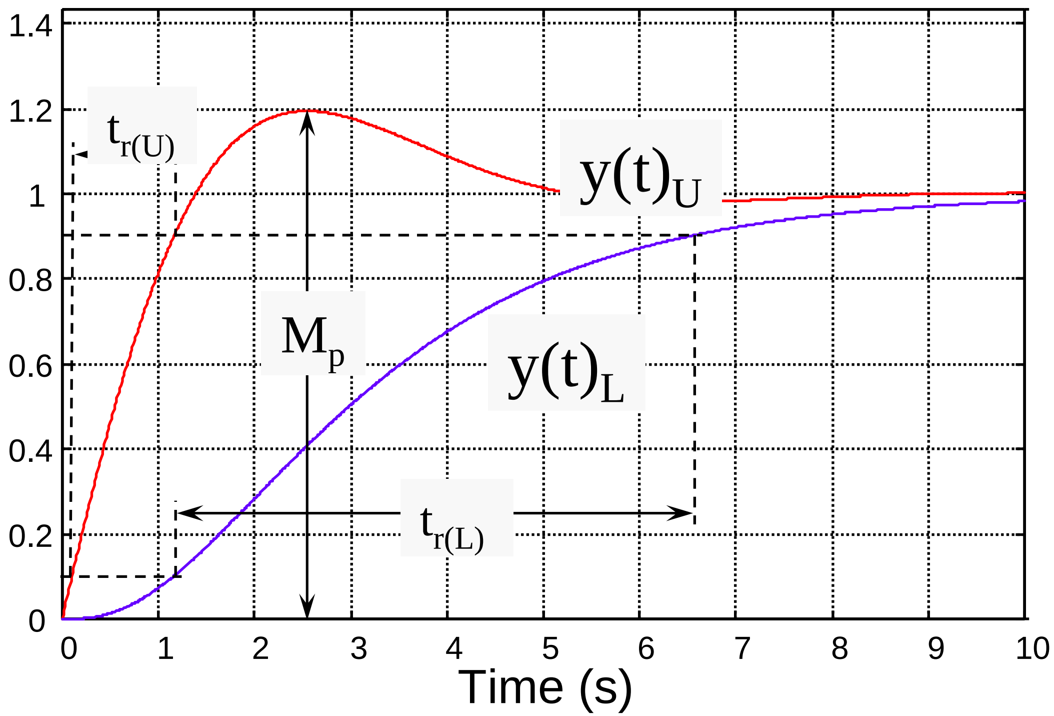

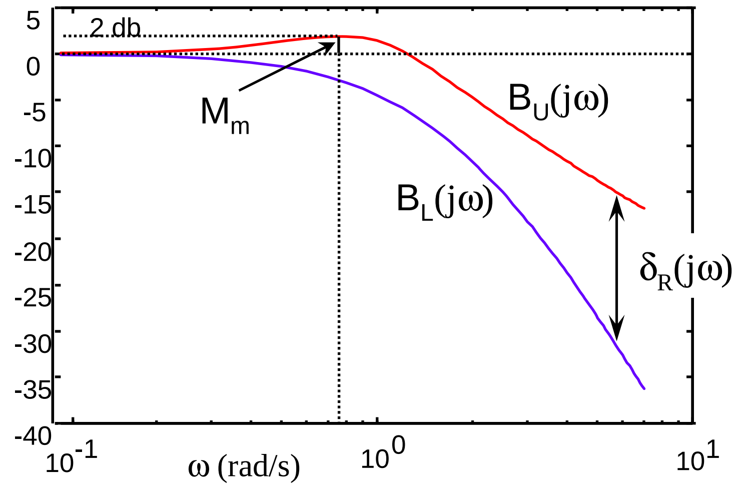

$\delta_R(j\omega) = B_U(j\omega) - B_L(j\omega)$
closed loop

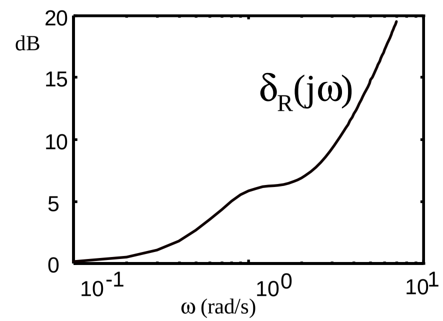

Mario Garcia-Sanz

Disturbance rejection

$$\left|\frac{1}{1+PGH}\right| \le W_{s2}$$

- **<u>Frequency-Domain Specifications:</u>** Desire TF system Y(ω)/U(ω) to lie under a specific bound, B(ω)

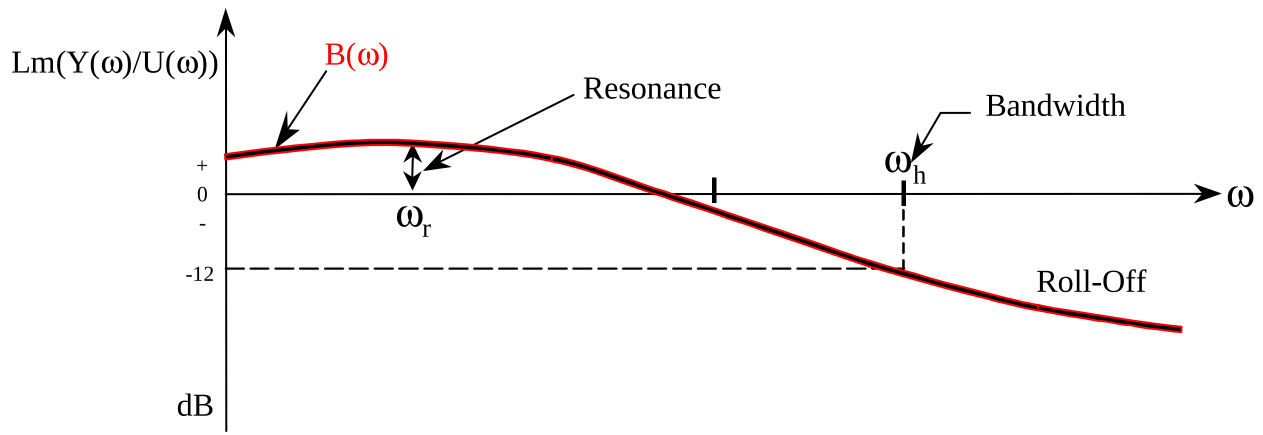

<u>Figures of merit</u> (FOM),

➔ Resonance; Bandwidth; Roll-off; Low Frequency, etc.

<u>Depends on</u> *requirements* that the designer wants for the *specific Plant*:

➔ Structure resonance, Noise measurement, Disturbances, Steady State Errors, etc...

Mario Garcia-Sanz

Disturbance rejection

$$\left| \frac{1}{1+PGH} \right| \leq W_{s2}$$

$$W_{s2} = T_d = \frac{1}{1+PGH} \leq \frac{s^2 + 2\xi\omega_n s}{s^2 + 2\xi\omega_n s + \omega_n^2}$$

Disturbance rejection

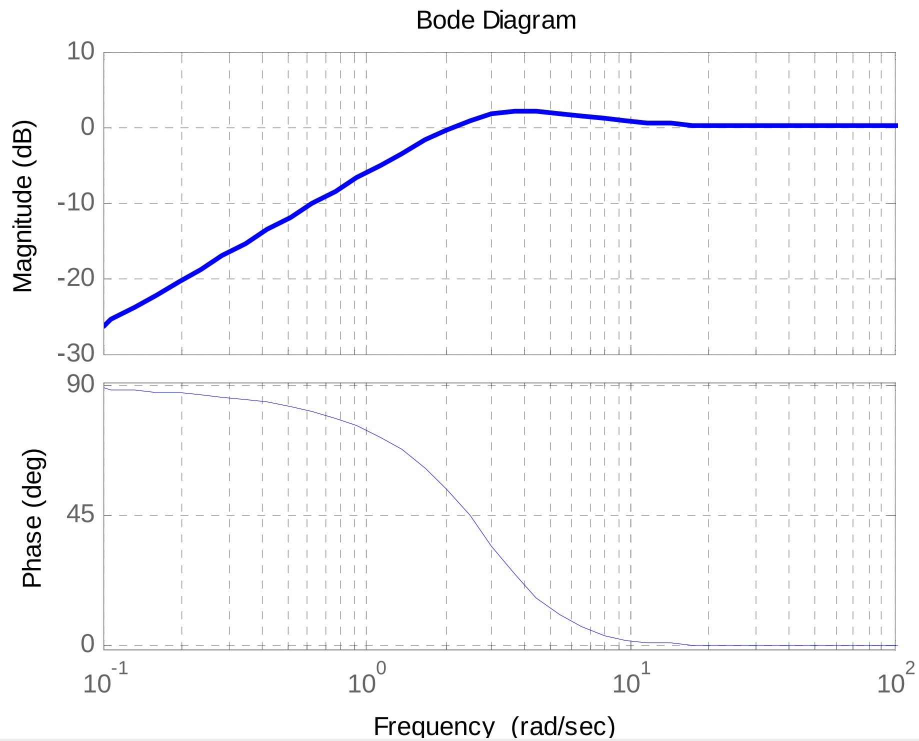

Mario Garcia-Sanz

Closed loop specifications are usually described in terms of frequency functions $\delta_k(\omega)$ that are imposed on the magnitude of the system transfer functions $|T_k|$, $k = 1, \dots 5$

(1) robust stability, control effort limit in the input disturbance rejection, sensor noise attenuation

(2) output system disturbance rejection

(3) input system disturbance rejection

(4) control effort limit in the output disturbance rejection, noise attenuation, and tracking

(5) signal tracking

Transfer functions and specifications	Eq.No.
$\lvert T_1(j\omega)\rvert = \left\lvert\frac{Y(j\omega)}{R(j\omega)\cdot F(j\omega)}\right\rvert = \left\lvert\frac{U(j\omega)}{D_1(j\omega)}\right\rvert = \left\lvert\frac{Y(j\omega)}{N(j\omega)}\right\rvert = \left\lvert\frac{P(j\omega)\cdot G(j\omega)}{1+P(j\omega)\cdot G(j\omega)}\right\rvert \le \delta_1(j\omega),\ \omega\in\{\omega_1\}$	(T1)
$\lvert T_2(j\omega)\rvert = \left\lvert\frac{Y(j\omega)}{D_2(j\omega)}\right\rvert = \left\lvert\frac{1}{1+P(j\omega)\cdot G(j\omega)}\right\rvert \le \delta_2(\omega),\ \omega\in\{\omega_2\}$	(T2)
$\lvert T_3(j\omega)\rvert = \left\lvert\frac{Y(j\omega)}{D_1(j\omega)}\right\rvert = \left\lvert\frac{P(j\omega)}{1+P(j\omega)\cdot G(j\omega)}\right\rvert \le \delta_3(\omega),\ \omega\in\{\omega_3\}$	(T3)
$\lvert T_4(j\omega)\rvert = \left\lvert\frac{U(j\omega)}{D_2(j\omega)}\right\rvert = \left\lvert\frac{U(j\omega)}{N(j\omega)}\right\rvert = \left\lvert\frac{U(j\omega)}{R(j\omega)\cdot F(j\omega)}\right\rvert = \left\lvert\frac{G(j\omega)}{1+P(j\omega)\cdot G(j\omega)}\right\rvert \le \delta_4(\omega),\ \omega\in\{\omega_4\}$	(T4)
$\delta_{5\inf}(\omega) \le \lvert T_5(j\omega)\rvert = \left\lvert\frac{Y(j\omega)}{R(j\omega)}\right\rvert = \left\lvert F(j\omega)\frac{P(j\omega)\cdot G(j\omega)}{1+P(j\omega)\cdot G(j\omega)}\right\rvert \le \delta_{5\sup}(\omega),\ \omega\in\{\omega_5\}$	(T5)

Mario Garcia-Sanz

Step 3: Plant Model + Uncertainty

Why Uncertainty?

Test-bed for Large Multipole Generators

Up to four 500 kW Motors drives a 3000 kW Generator

A Simple Mathematical Description

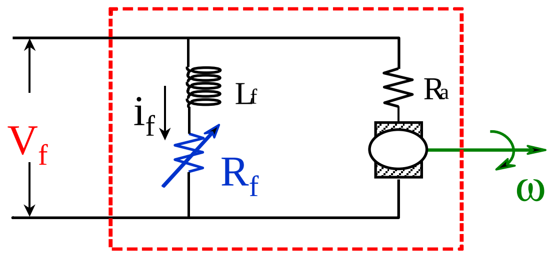

Motor transfer function is:

$$P_\iota(s) = \frac{\Theta_m(s)}{V_f(s)} = \frac{Ka}{s(s+a)}$$

Parameters K and a vary: $K \in (K_{min}, K_{max})$

and $a \in (a_{min}, a_{max})$

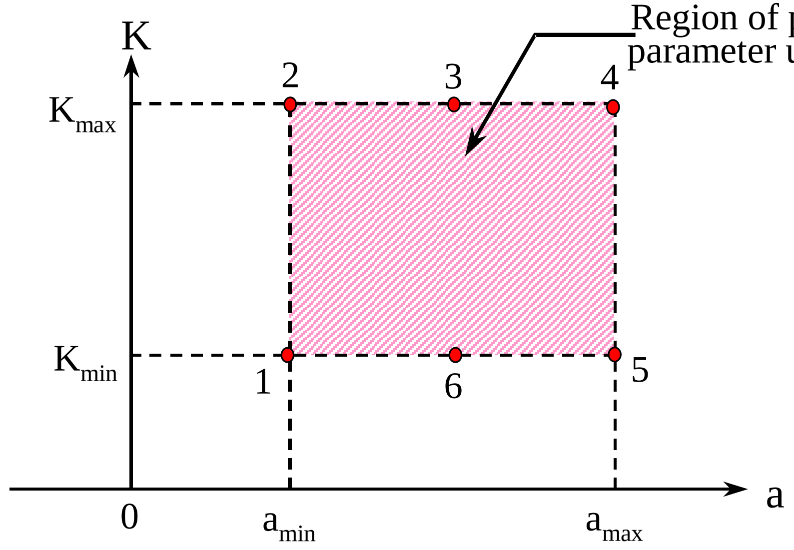

Region of plant parameter uncertainty.

Shaded region represents the region of plant uncertainty.

Motor represented by 6 LTI transfer functions P_ι ($\iota = 1,2,\ldots,J$).

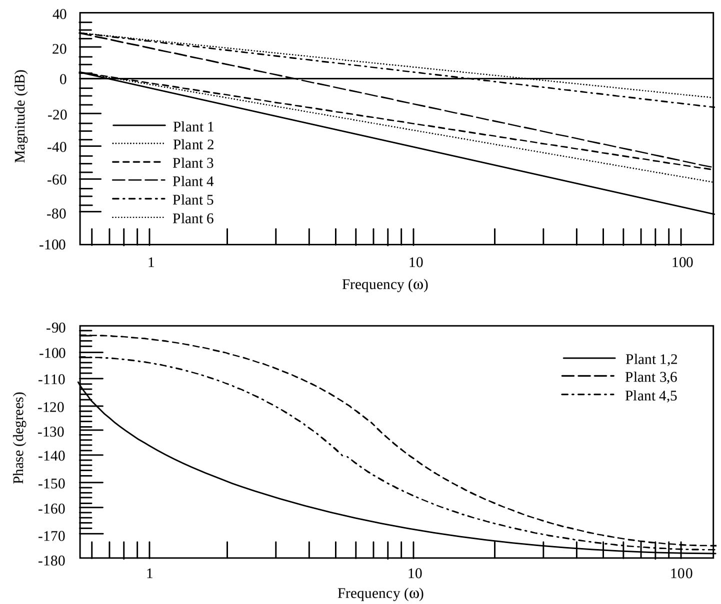

Mario Garcia-Sanz

Step 4: Templates

- Plant Template obtained by mapping
  Points of uncertainty region
  into points on to the N.C.
  Curve drawn through points –
  Shaded area labeled $\Im \boldsymbol{P}(j1)$

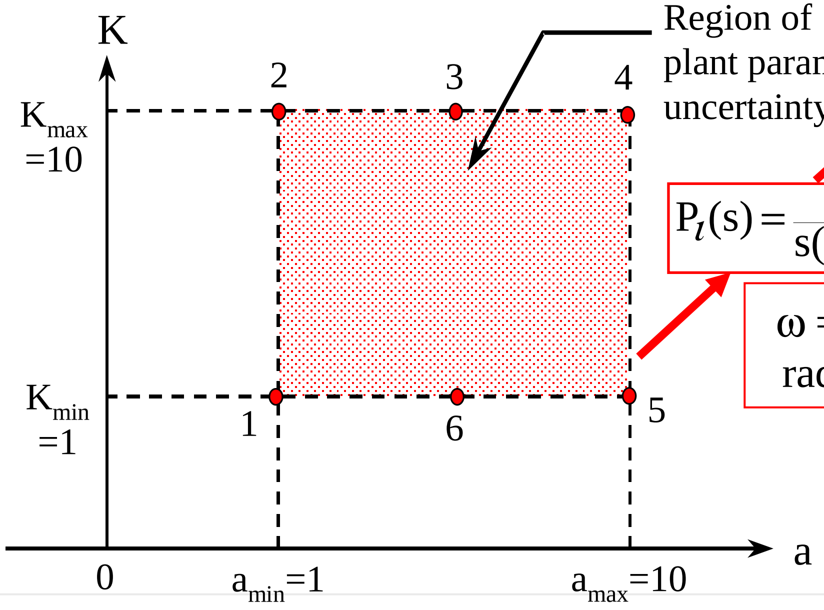

$$P_l(s) = \frac{Ka}{s(s+a)}$$

$\omega = 1$ rad/s

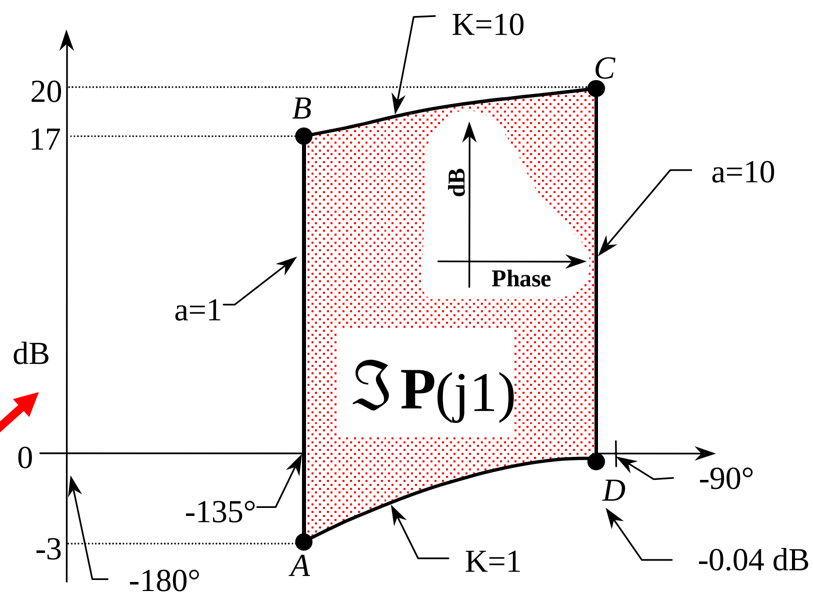

N.C. characterizing P(s) over the region of uncertainty.

Mario Garcia-Sanz

- Templates for other values of ω_i are obtained

- <u>Characteristic of templates</u>:

  ➔ Starting from low values of ω_i, (narrow width),the angular width becomes larger (medium freq.)

  ➔ For increasing values of ω_i templates become narrower again.

  ➔ Eventually approach straight line: height V dB

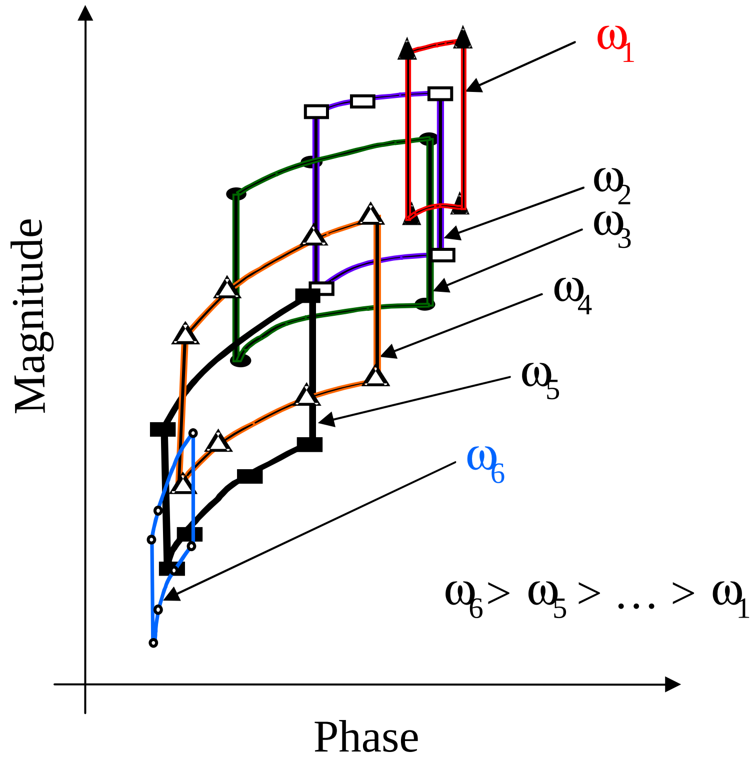

$$\Delta = \lim_{\omega \to \infty} [20 \log_{10} P_{max} - 20 \log_{10} P_{min}] = 20 \log_{10} K_{max} - 20 \log_{10} K_{min} = V \text{ dB}$$

Mario Garcia-Sanz

Example: *4-dimensional parameter space*

$$\mathbf{P}_1 = \left\{ \begin{array}{l} P_1(s) = \dfrac{k}{a\ s + b}\ \exp(-\tau s) \\ a \in [1,\ 5],\ b \in [10,\ 12], \\ k \in [1,\ 2],\ \tau \in [0.1,\ 0.2] \end{array} \right\}$$

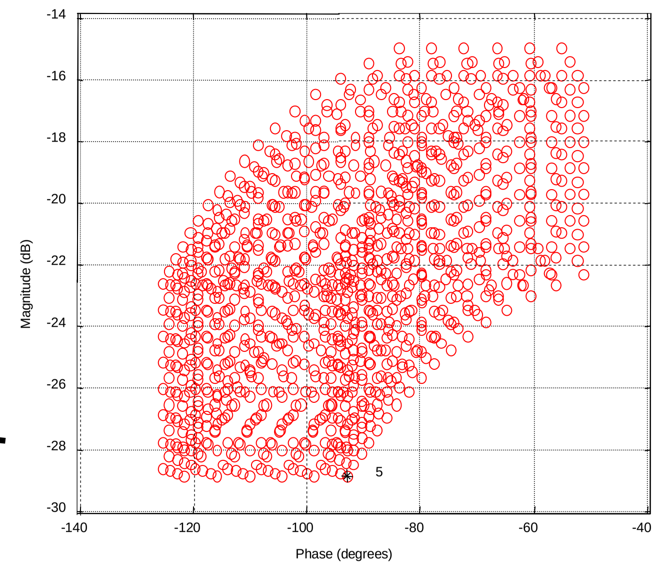

Whole Template

Ω_4

for $\omega = 5$ rad/sec

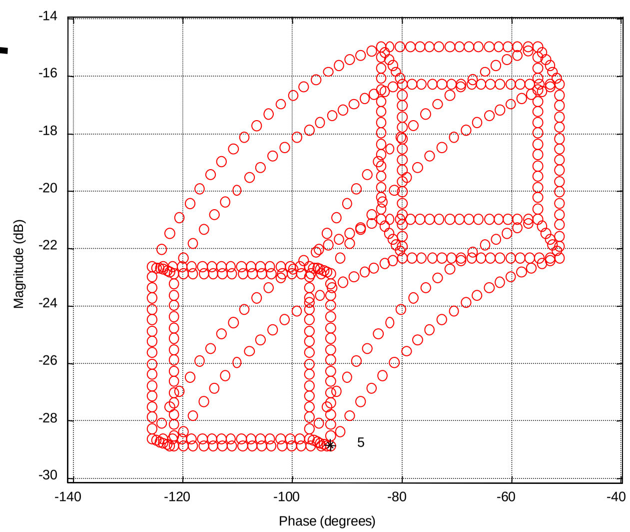

Edges Template

Ω_1

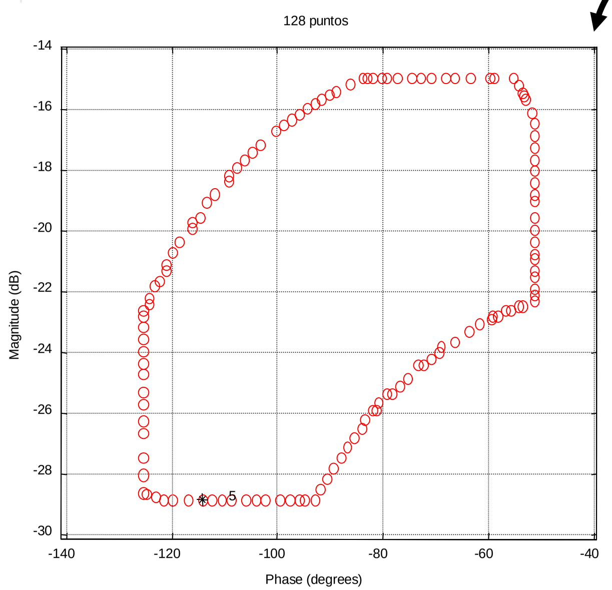

Contour Template

Mario Garcia-Sanz

Step 5: Nominal Plant

- Chose any plant
- Keep the same plant (set of parameters) as the nominal for all frequencies

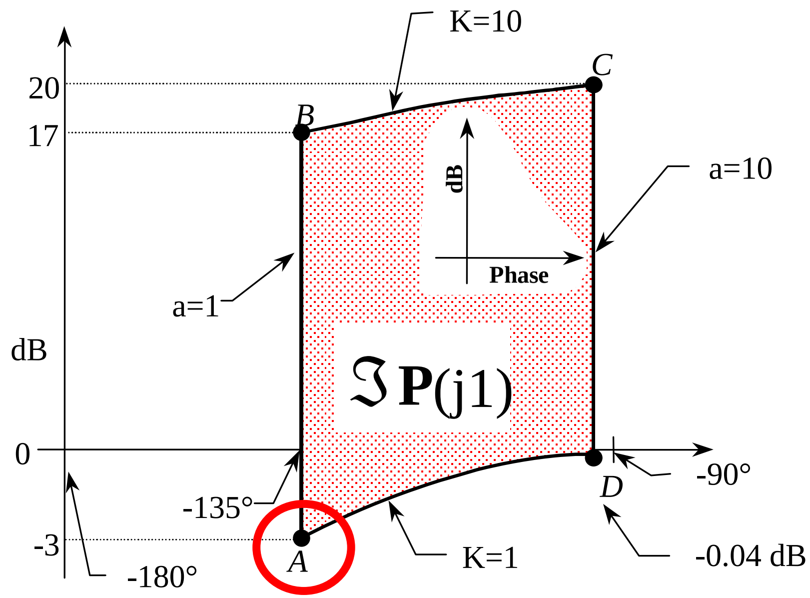

Mario Garcia-Sanz

Step 6: U-Contour (Stability bounds)

The Forbidden Region is extended by V dB.

$$P(s) = K \frac{\prod_{i=1}^{m}(s+z_i)}{\prod_{i=1}^{n}(s+p_i)} \xrightarrow{\omega \to \infty} \frac{K}{s^{n-m}}$$

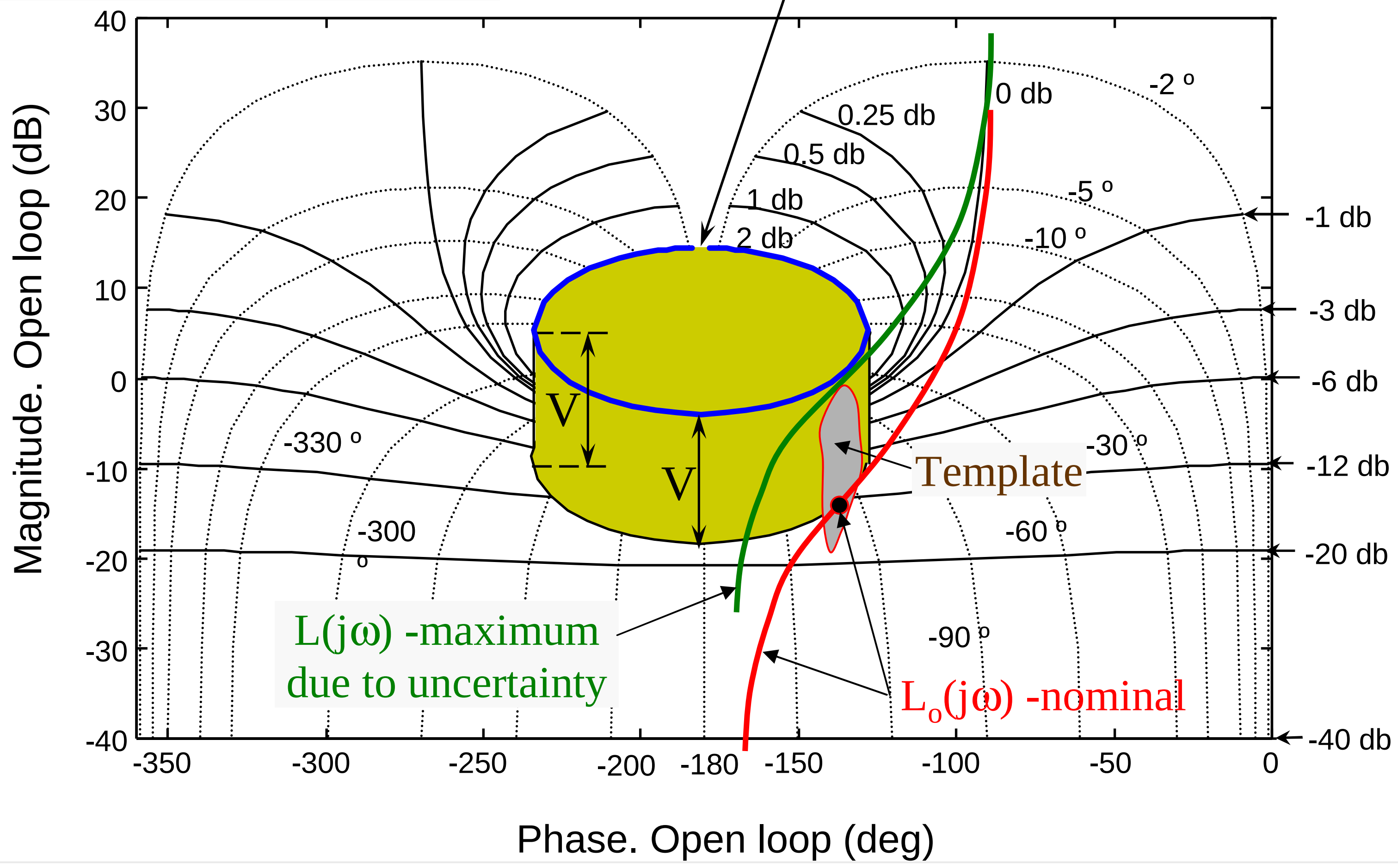

Mario Garcia-Sanz

Step 7: Tracking Bounds on L_o

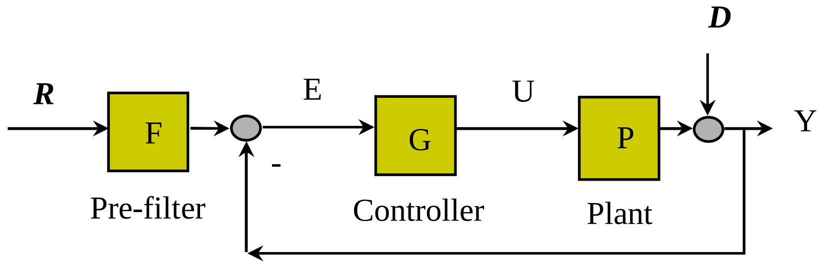

Upper function $T_{RU} = \dfrac{(\omega_n^2/a)(s+a)}{s^2+2\xi\omega_n s+\omega_n^2}$

Lower function $T_{RL} = \dfrac{k}{(s+\sigma_1)(s+\sigma_2)(s+\sigma_3)}$

$y(t)_U$. ($\omega_n = 1$; $a = 1$; $\xi = 0.6$)

$y(t)_L$. ($\sigma_1 = 0.5$; $\sigma_2 = 1$; $\sigma_3 = 2$; $k = 1$)

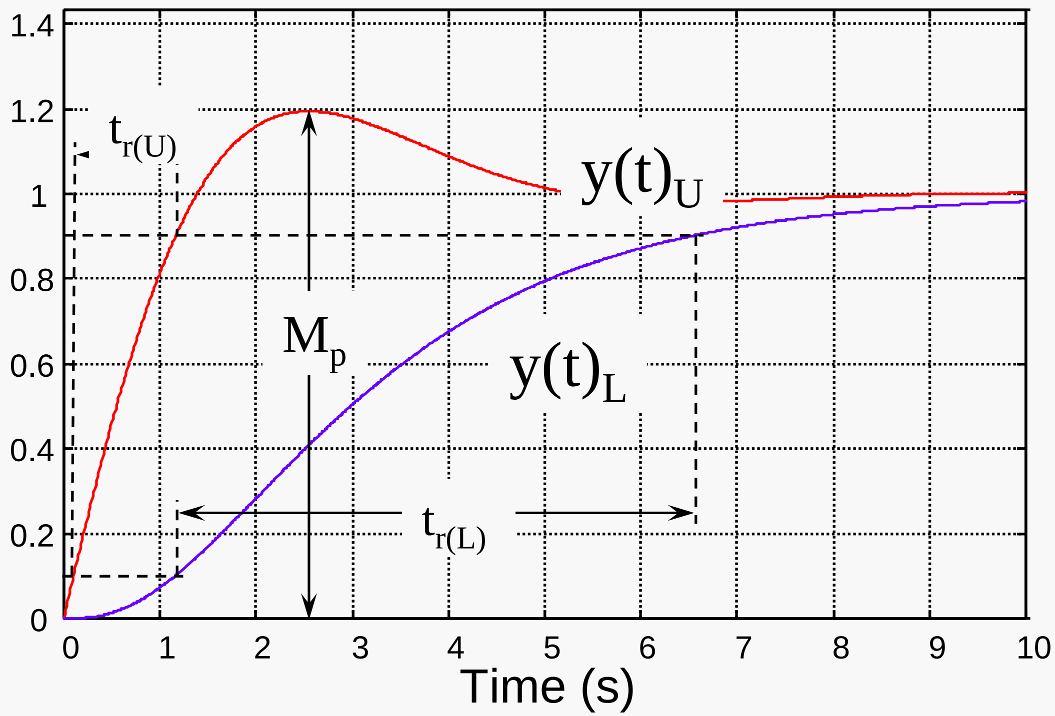

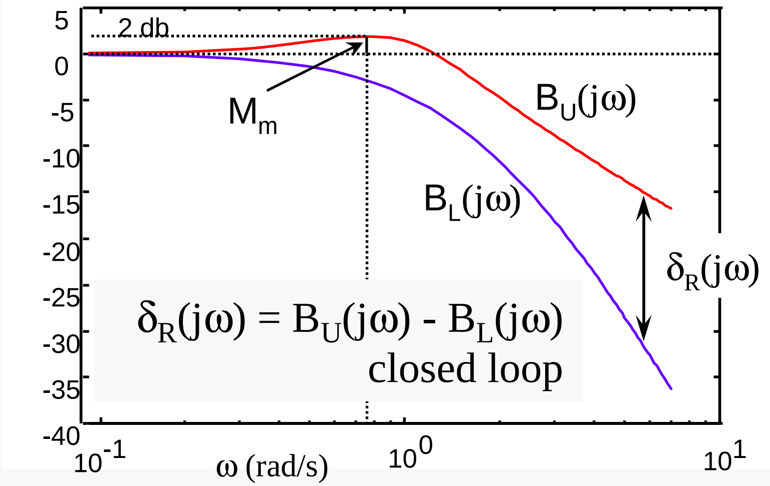

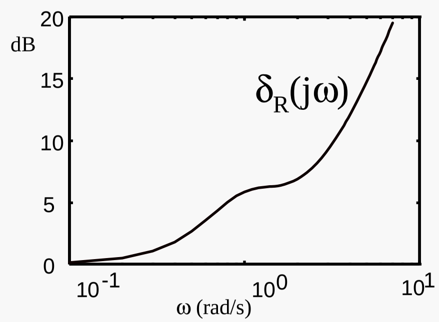

ario Garcia-Sanz

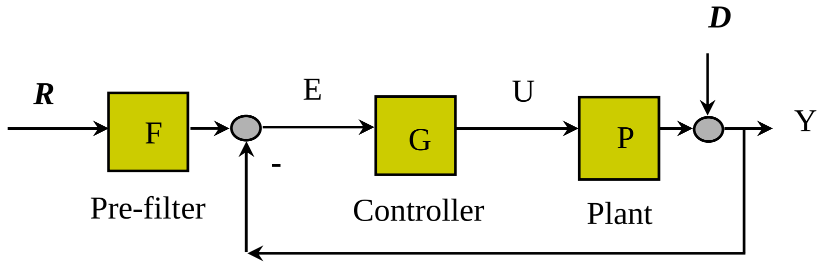

- Solution for $\mathbf{B}_R(j\omega_i)$ requires:
  $\Delta T_R(j\omega_i) \le \delta_R(j\omega_i) = B_U(j\omega_i) - B_L(j\omega_i)$ dB
  be satisfied for all $\mathbf{L}_\iota(j\omega_i)$.

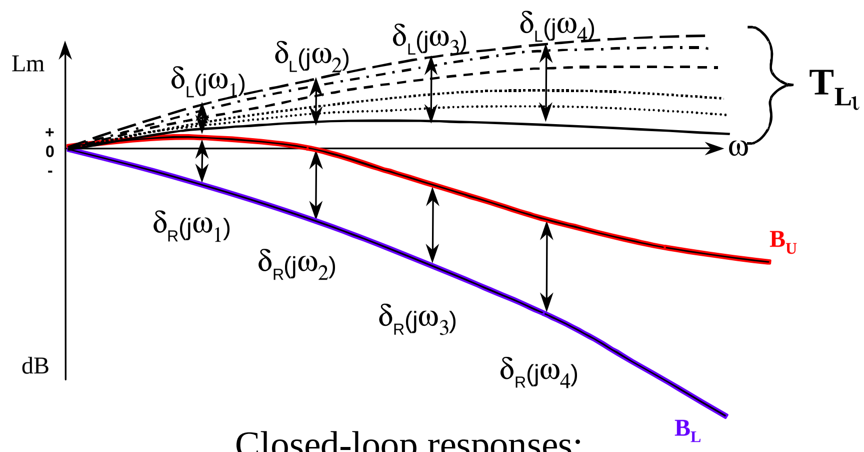

- And $\Delta T_R(j\omega_i)$
  are between B_U and B_L

Closed-loop responses:
LTI plants with **only G(s)**

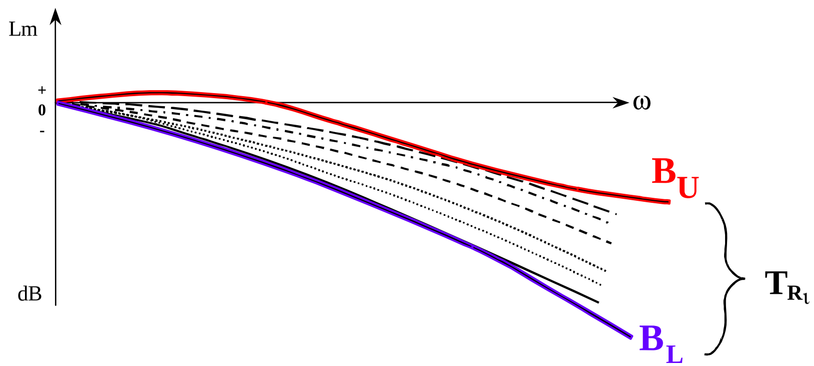

Closed-loop responses:
LTI plants **with G(s) and F(s)**

Mario Garcia-Sanz

The classic graphical procedure

Based on the nominal plant
At specified ω_i
By use of templates
Along every NC phase grid line

Repeat procedure on sufficient **phase grid** lines to provide enough points to draw $B_R(\omega_i)$

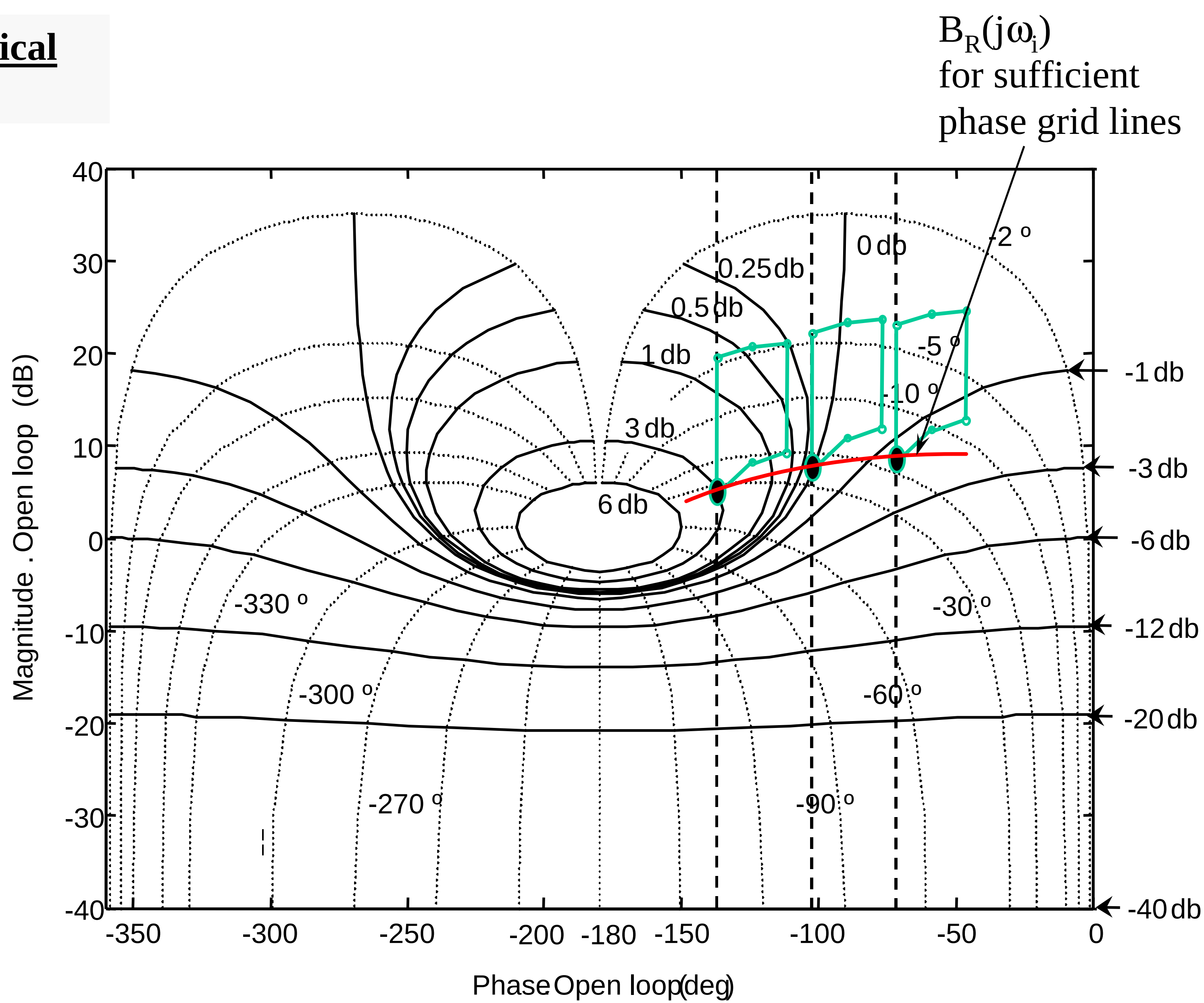

Mario Garcia-Sanz

Step 8: Disturbance Rejection Bounds

- Case 1 Disturbance at Plant Output [$d_2(t) = D_o u_{-1},(t)$, $d_1(t) = 0$] the disturbance control ratio for input $d_2(t)$ is,

$$T_{D2}(s) = \frac{Y(s)}{D_2(s)} = \frac{1}{1+L}$$

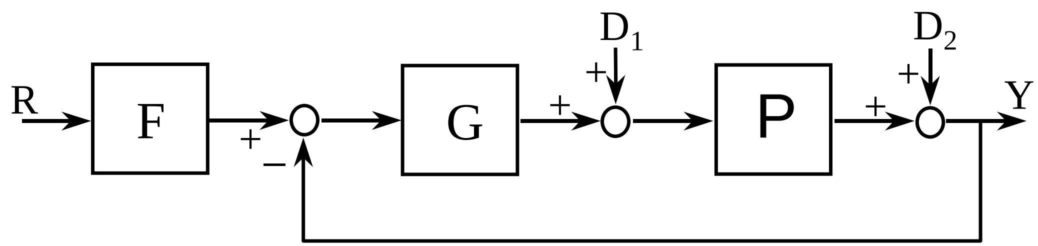

A 2DOF feedback structure.

Substituting $L = G\,P = 1/l$ yields

$$T_{D2}(s) = \frac{Y(s)}{D_2(s)} = \frac{\ell}{1+\ell}$$

which has the mathematical format required to use the N.C.

A N.C.

is rotated 180º

Change of sign of the vertical axis in dB, and horizontal axis in deg.

Similar that used for the tracking bounds

Now looking for:

$$20\log_{10} T_{D2}(j\omega_i) =$$

$$= 20\log_{10}\left|\frac{\mathbf{Y}(j\omega)}{\mathbf{D}_2(j\omega)}\right| = 20\log_{10}\left|\frac{1}{1+L}\right| =$$

$$= 20\log_{10}\left|\frac{(1/L)}{1+(1/L)}\right| \le \delta_{D2}(j\omega_i)\,\mathrm{dB}$$

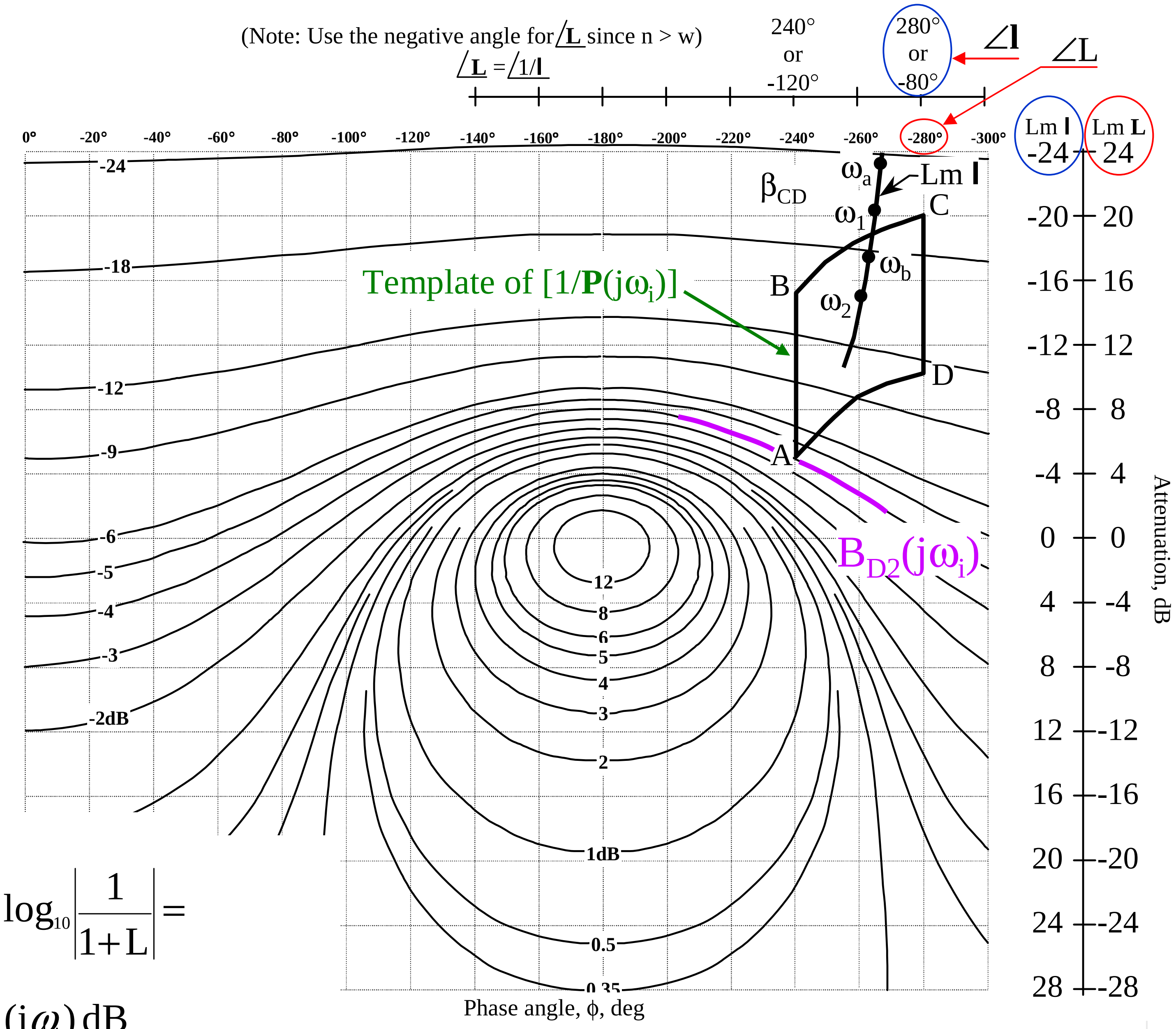

Rotated Nichols chart.

Mario Garcia-Sanz

Inequalities Bounds Expressions (Steps 6 to 8)

The modern procedure

Let's consider the two-degrees-of-freedom feedback system.

In a general real-world problem *P(s)* will present uncertainty $\{P\}$.

The compensator *G(s)* and a the pre-filter *F(s)* will be designed to meet robust stability and robust performance specifications,

and to deal with references *R(s)*, disturbances $D_{1,2}(s)$, signal noise *N(s)* and saturable control effort *U(s)*,

minimizing the 'cost of the feedback' (excessive bandwidth)

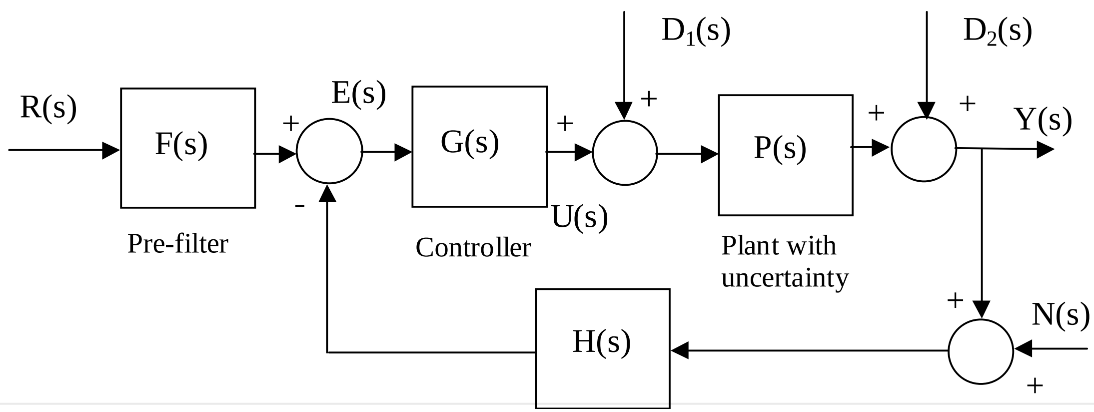

Mario Garcia-Sanz

Closed loop specifications are usually described in terms of frequency functions $\delta_k(\omega)$ that are imposed on the magnitude of the system transfer functions $|T_k|$, $k = 1, \dots 5$

(1) robust stability, control effort limit in the input disturbance rejection, sensor noise attenuation

(2) output system disturbance rejection

(3) input system disturbance rejection

(4) control effort limit in the output disturbance rejection, noise attenuation, and tracking

(5) signal tracking

Transfer functions and specifications	Eq.No.
$\lvert T_1(j\omega)\rvert = \left\lvert \frac{Y(j\omega)}{R(j\omega)\cdot F(j\omega)} \right\rvert = \left\lvert \frac{U(j\omega)}{D_1(j\omega)} \right\rvert = \left\lvert \frac{Y(j\omega)}{N(j\omega)} \right\rvert = \left\lvert \frac{P(j\omega)\cdot G(j\omega)}{1+P(j\omega)\cdot G(j\omega)} \right\rvert \le \delta_1(j\omega),\ \omega\in\{\omega_1\}$	(1)
$\lvert T_2(j\omega)\rvert = \left\lvert \frac{Y(j\omega)}{D_2(j\omega)} \right\rvert = \left\lvert \frac{1}{1+P(j\omega)\cdot G(j\omega)} \right\rvert \le \delta_2(\omega),\ \omega\in\{\omega_2\}$	(2)
$\lvert T_3(j\omega)\rvert = \left\lvert \frac{Y(j\omega)}{D_1(j\omega)} \right\rvert = \left\lvert \frac{P(j\omega)}{1+P(j\omega)\cdot G(j\omega)} \right\rvert \le \delta_3(\omega),\ \omega\in\{\omega_3\}$	(3)
$\lvert T_4(j\omega)\rvert = \left\lvert \frac{U(j\omega)}{D_2(j\omega)} \right\rvert = \left\lvert \frac{U(j\omega)}{N(j\omega)} \right\rvert = \left\lvert \frac{U(j\omega)}{R(j\omega)\cdot F(j\omega)} \right\rvert = \left\lvert \frac{G(j\omega)}{1+P(j\omega)\cdot G(j\omega)} \right\rvert \le \delta_4(\omega),\ \omega\in\{\omega_4\}$	(4)
$\delta_{5\,\inf}(\omega) \le \lvert T_5(j\omega)\rvert = \left\lvert \frac{Y(j\omega)}{R(j\omega)} \right\rvert = \left\lvert F(j\omega)\frac{P(j\omega)\cdot G(j\omega)}{1+P(j\omega)\cdot G(j\omega)} \right\rvert \le \delta_{5\,\sup}(\omega),\ \omega\in\{\omega_5\}$	(5)

Table 1

Each plant in the ω_i-template and the controller can be expressed in its polar form:

Plant $\quad P(j\omega_i) = \{P_r(j\omega_i) = p\angle\theta,\ r = 0,\ldots,m-1\}$

Controller $\quad \mathrm{G}(\mathrm{j}\omega_{\mathrm{i}}) = \mathrm{g}\angle\phi$

Then, substituting and rearranging the inequalities -Eq. (1) to (5) in Table 1-, they can be reduced to the quadratic inequalities –*k-problem* (1) to (5) in Table 2-.

Solving equalities such as $ag^2+bg+c = 0$ the set of **ω_i-bounds** for $\{\delta_{k=1,..,5}\}$ is computed.

k-problem	Bound Quadratic Inequality
1	$p^2 \cdot \left(1-\frac{1}{\delta_1^2}\right)\cdot g^2 + 2\cdot p\cdot\cos(\phi+\theta)\cdot g + 1 \ge 0$
2	$p^2 \cdot g^2 + 2\cdot p\cdot\cos(\phi+\theta)\cdot g + \left(1-\frac{1}{\delta_2^2}\right) \ge 0$
3	$p^2 \cdot g^2 + 2\cdot p\cdot\cos(\phi+\theta)\cdot g + \left(1-\frac{p^2}{\delta_3^2}\right) \ge 0$
4	$\left(p^2 - \frac{1}{\delta_4^2}\right)\cdot g^2 + 2\cdot p\cdot\cos(\phi+\theta)\cdot g + 1 \ge 0$
5	$p_e^2 p_d^2\left(1-\frac{1}{\delta_5^2}\right)\cdot g^2 + 2p_e p_d\left(p_e\cos(\phi+\theta_d) - \frac{p_d}{\delta_5^2}\cos(\phi+\theta_e)\right)\cdot g + \left(p_e^2 - \frac{p_d^2}{\delta_5^2}\right) \ge 0$

Table 2 $\qquad \delta_5 = \delta_{5sup}/\delta_{5inf}$

Mario Garcia-Sanz

Algorithm to compute the bounds

Y. Chait, and O. Yaniv, "Multi-input/single-output computer-aided control design using the Quantitative Feedback Theory," *Int. J. Robust & Non-linear Control*, vol.3, pp. 47-54, 1993.

1.	Discretize the domain $\{\omega_k\}$ into a finite set $\Omega_k = \{\omega_i \ , i=1,...,n\}_k$.
2.	Establish the uncertain LTI plant models $\wp = \{P(j\omega)\}$ and map its boundary for each frequency $\omega_i \in \Omega_k$ on the Nichols chart. A set of n templates $\{P(j\omega_i)\}$, $i=1,...,n$ is obtained. Each template $P(j\omega_i) = \{P_r(j\omega_i) = p\angle\theta, r=0,...,m-1\}$ contains m points or plants. Select one of them as the nominal plant $P_0(j\omega_i) = p_0\angle\theta_0$.
3.	Now, the conditions to meet by the controller $G(j\omega_i) = g\angle\phi$ have to be computed.
4.	Define a range, Φ, for the compensator's phase ϕ, and discretize it; for example $\phi \in \Phi = [-360^o : 5^o : 0^o]$.
5.	Choose a single frequency $\omega_i \in \Omega_k$.
6.	Choose a single controller's phase $\phi \in \Phi$.
7.	Choose a single plant in the ω_i-template: $P_r(j\omega_i) = p\angle\theta$.
8.	At this step, the k feedback problem is reduced to solve a k quadratic inequality without uncertainty. The feedback problems in equations (1) to (5) in Table I are reduced to inequalities in Table II.
9.	Compute the maximum $g_{max} = g_{max}(P_r)$ and the minimum $g_{min} = g_{min}(P_r)$ of the two roots g_1 and g_2 that solve the k quadratic inequality,.
10.	Repeat Steps 6 and 7 for the m plants $P_r(j\omega_i), r=0,...m-1$ in the ω_i template $P(j\omega_i)$.
11.	Choose the most restrictive of the m $g_{max}(P_r)$ and the m $g_{min}(P_r)$. Thus, $g_{max}(P)$ and $g_{min}(P)$ are obtained. They are the maximum and minimum bound points for the controller magnitude g at a phase ϕ.
12.	Repeat Step 5 over the range Φ. The union of $g_{max}(P)$ and $g_{min}(P)$ for each $\phi \in \Phi$ gives $g_{max}\angle\phi$ and $g_{min}\angle\phi$, respectively.
13.	Now the bounds for the open loop transmission $L_0(j\omega_i) = l_0\angle\psi_0$ are computed. Set $l_{0max}\angle\psi_0 = p_0 \cdot g_{max}\angle\phi$ and $l_{0min}\angle\psi_0 = p_0 \cdot g_{min}\angle\phi$, being $\psi_0 = \phi + \theta_0$, $\phi = [-360^o : 5^o : 0]$. These bounds will be labelled $B_k(j\omega_i)$.
14.	Repeat Step 4 over the range Ω_k . The set of bounds for the k c ontrol problem $\{B_k(j\omega_i), \omega_i \in \Omega_k\}$ has just been computed.

The set of ω_i-bounds

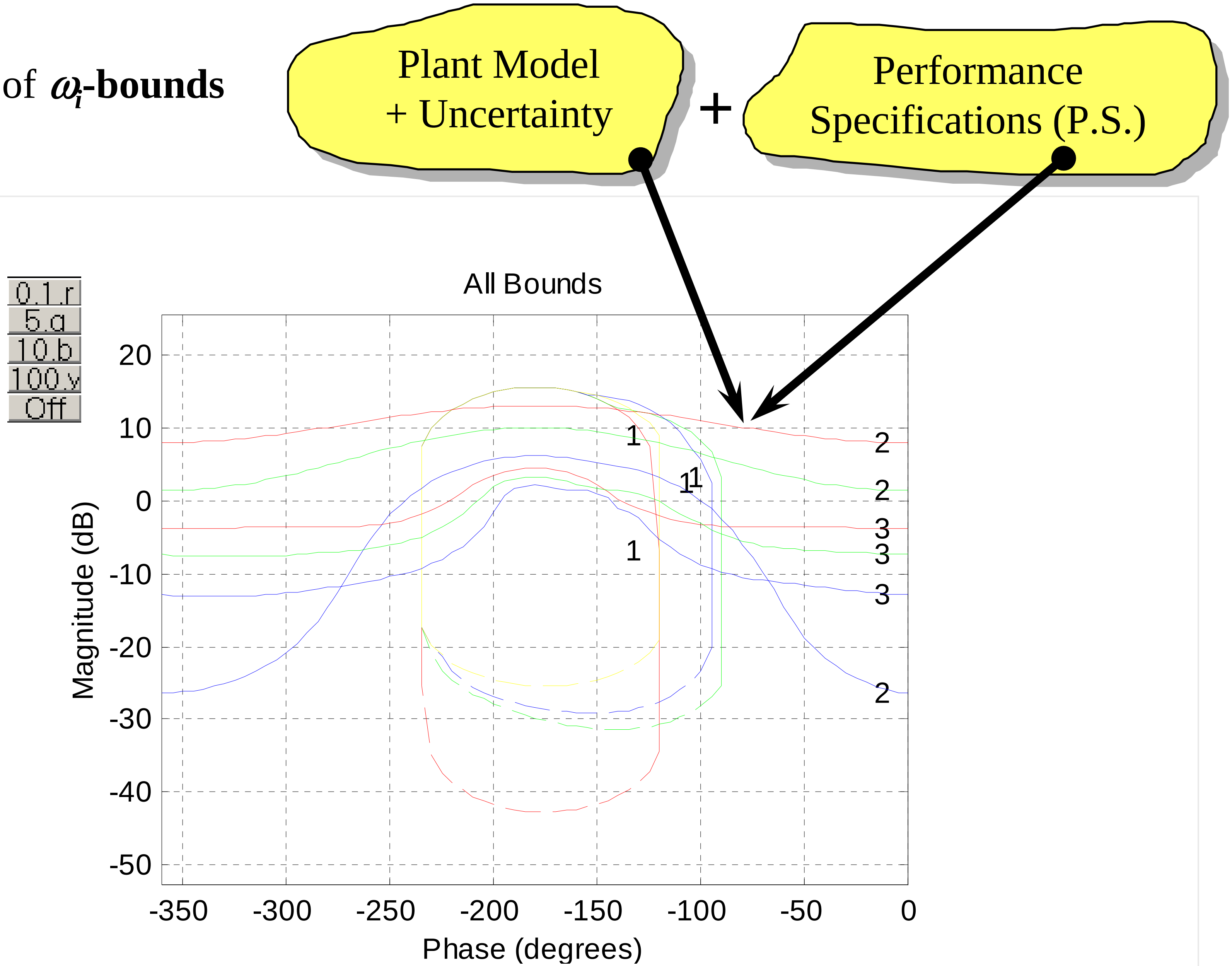

Mario Garcia-Sanz

Step 9: Optimal Bounds $B_o(j\omega_i)$

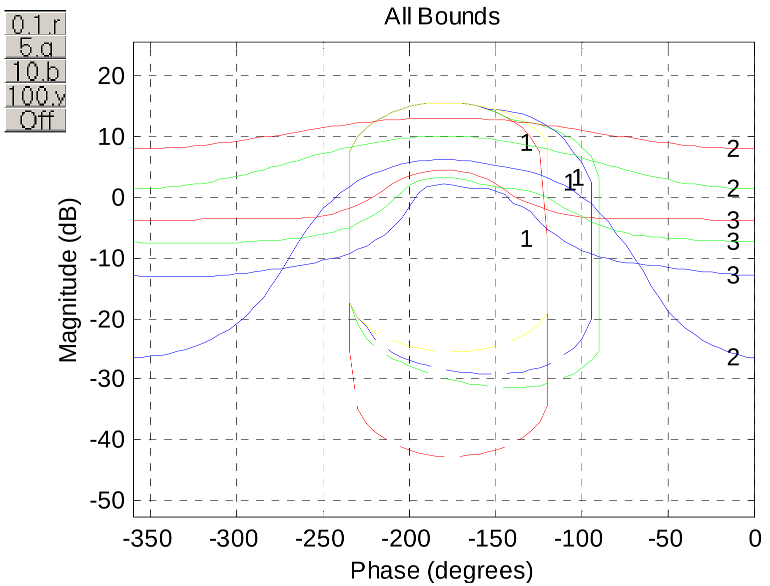

Intersection of ω_i-bounds

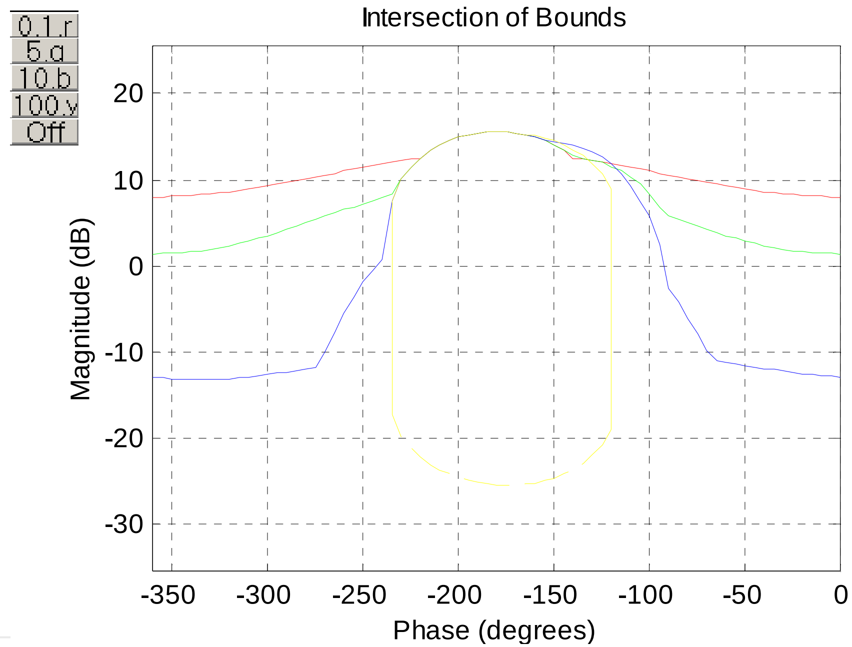

One line for each frequency ω_i

The most demanding one

Mario Garcia-Sanz

Step 10: Synthesizing G(s)
or Loop Shaping $L_o(s)$

- Shaping of $L_o(j\omega) = P_o(j\omega)\, G(j\omega)$
  Only one $L = L_o$ to be shape!!

- $\mathbf{L_o}(j\omega_i)$ must be at every ω_i:
  - outside the U-contour
  - above the continuous bounds $B_0(j\omega)$
  - below the discont. Bounds $B_0(j\omega)$

- Synthesize rational function $L_o(s)$
  Build up $G(j\omega)$ term-by-term adding some elements like: gain, real poles and zeros, complex poles and zeros, integrators, differentiators, lead/lag networks, notch filters, second order TF, etc.

- Compensator: $G(s) = L_o(s)/P_o(s)$

- Probably one of the most difficult steps of the methodology for the beginner.

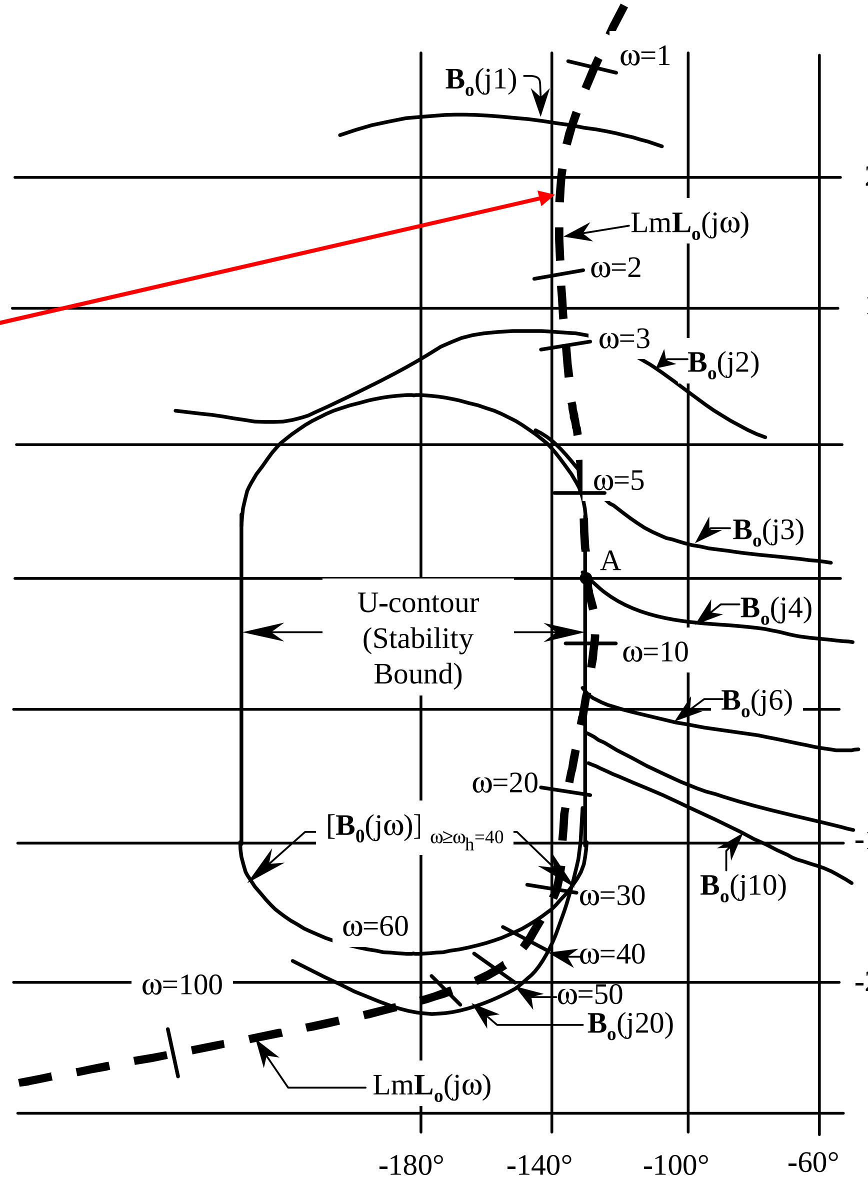

Mario Garcia-Sanz

Procedure:

Build up $L_o(j\omega) = P_o(j\omega)\left(K \prod_{i=0}^{n} [G_i(j\omega)]\right)$ term-by-term adding some elements like:

1. Gain k
2. Real Pole $\dfrac{1}{\frac{s}{p}+1}$
3. Real Zero $\dfrac{s}{z}+1$
4. Complex Pole $\dfrac{1}{\frac{s^2}{\omega_n^2}+\frac{2\zeta s}{\omega_n}+1}$ $(\zeta<1)$
5. Complex Zero $\dfrac{s^2}{\omega_n^2}+\dfrac{2\zeta s}{\omega_n}+1$ $(\zeta<1)$
6. 2º order / 2º order $\dfrac{a_1 s^2 + a_2 s + 1}{b_1 s^2 + b_2 s + 1}$
7. Integrator $\dfrac{1}{s^n}$
8. Differenciator s^n
9. Lead/Lag Network $\dfrac{\frac{s}{z}+1}{\frac{s}{p}+1}$
10. Notch Filter $\dfrac{\frac{s^2}{\omega_n^2}+\frac{2\zeta_1 s}{\omega_n}+1}{\frac{s^2}{\omega_n^2}+\frac{2\zeta_2 s}{\omega_n}+1}$

etc...

Mario Garcia-Sanz

The Interactive Design Environment (IDE): (Terasoft, version 2)

Interactive tool to design the controller G(s)

Function:

lpshape(...)

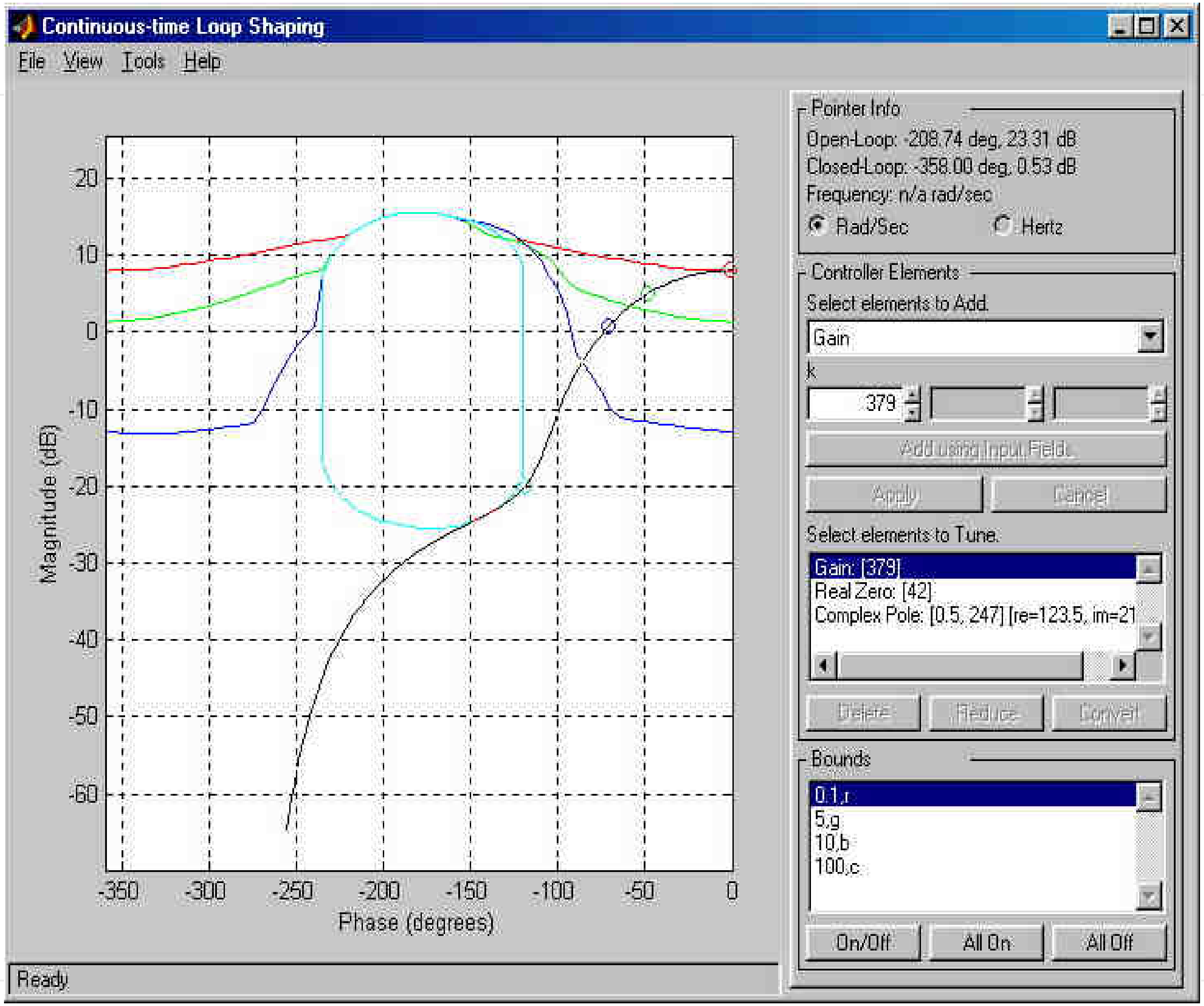

Only one

$L = L_o$

to be shape!!

&

the controller is for the whole set of uncertain plants

Controller design

Step 11: Prefilter Design F(s)

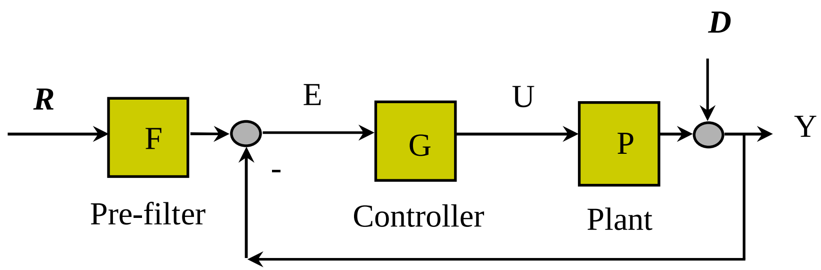

to lie between $\mathbf{B}_U$ & $\mathbf{B}_L$ for all J plants

$\Rightarrow$ A Prefilter F(s) is needed

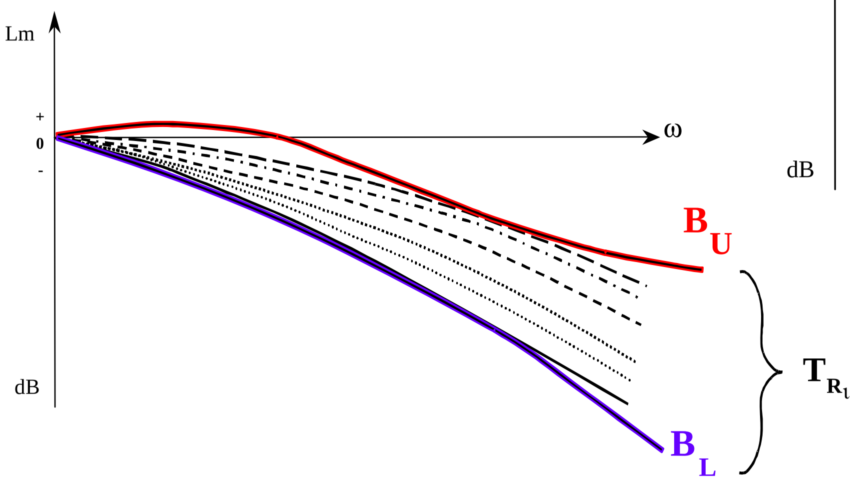

Fig. 10 Closed-loop responses: LTI plants **with G(s) and F(*s*)**

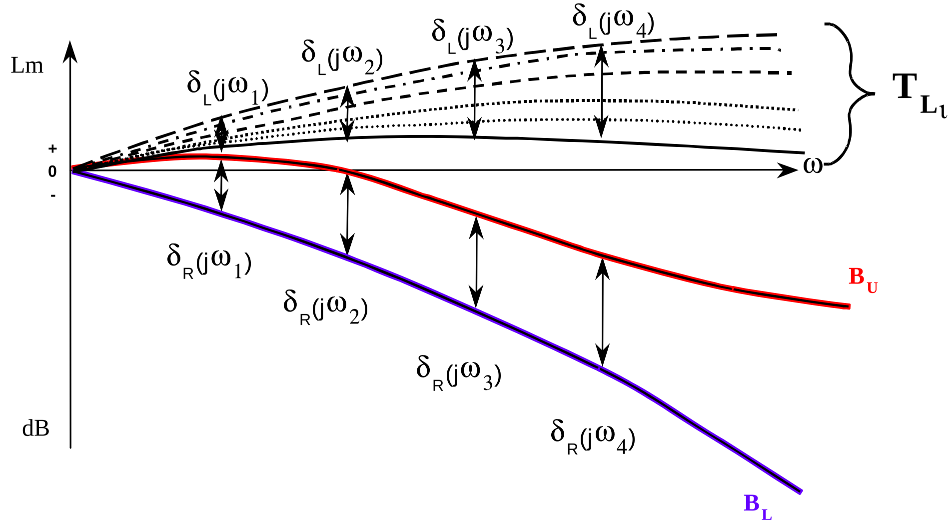

Fig. 9 Closed-loop responses: LTI plants with **only G(s)**

Mario Garcia-Sanz

$$\begin{cases} Lm\,T_{RU} - Lm\,T_{max} = B_U - Lm\,T_{max} = Lm\,F_{max} \\ Lm\,T_{RL} - Lm\,T_{min} = B_L - Lm\,T_{min} = Lm\,F_{min} \end{cases}$$

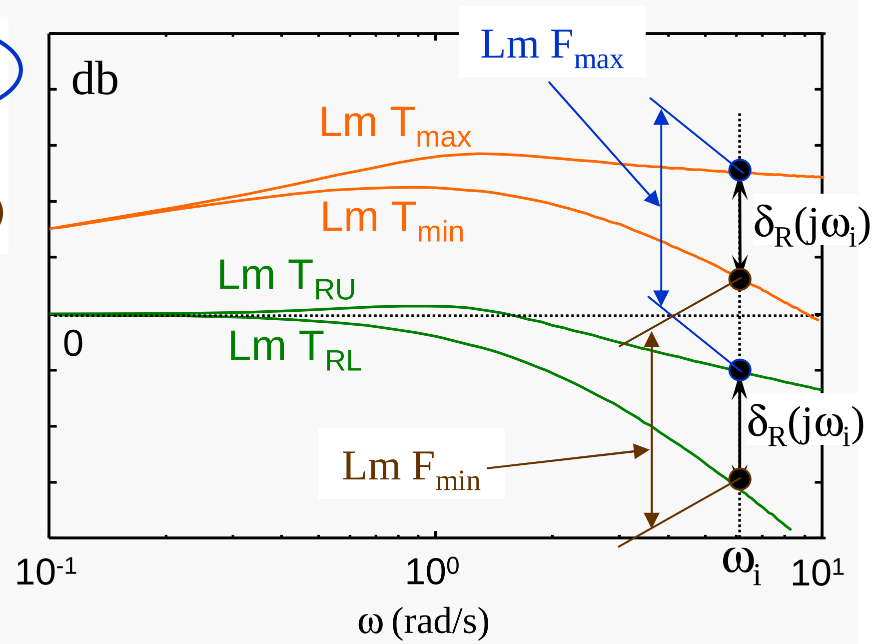

We have to move down more than F_{max} but less than F_{min}.

$$Lm\,F_{max}(j\omega) < Lm\,F(j\omega) < Lm\,F_{min}(j\omega)$$

$$\lim_{s \to 0} F(s) = 1$$

F(s) is synthesized,
in dashes,
that lies within
the upper & lower
plots

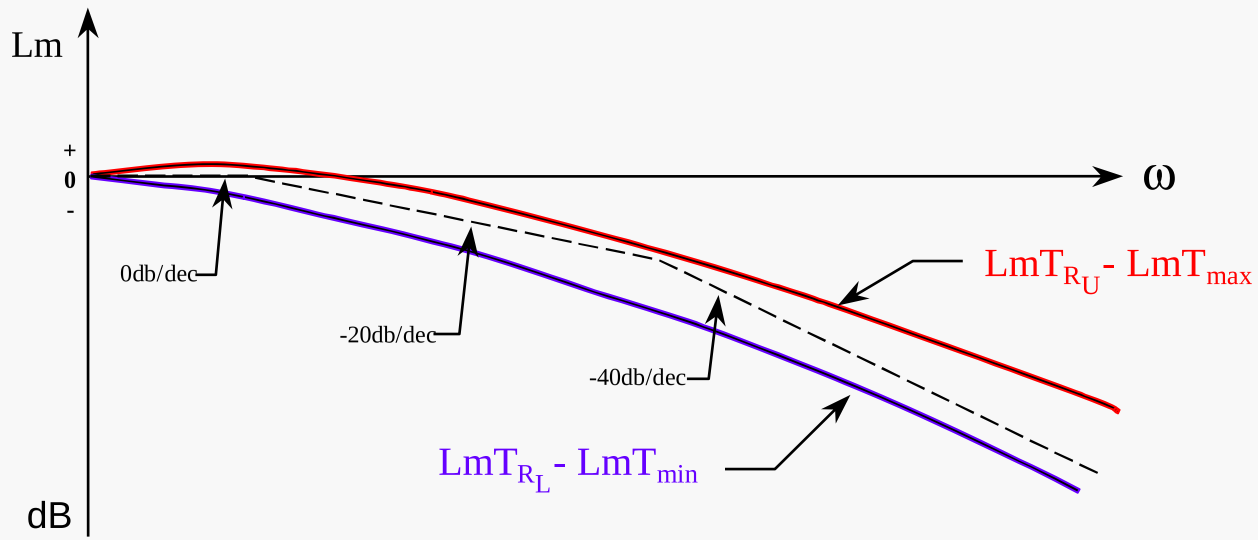

Frequency bounds on the prefilter F(s).

Mario Garcia-Sanz

(Terasoft, version 2)

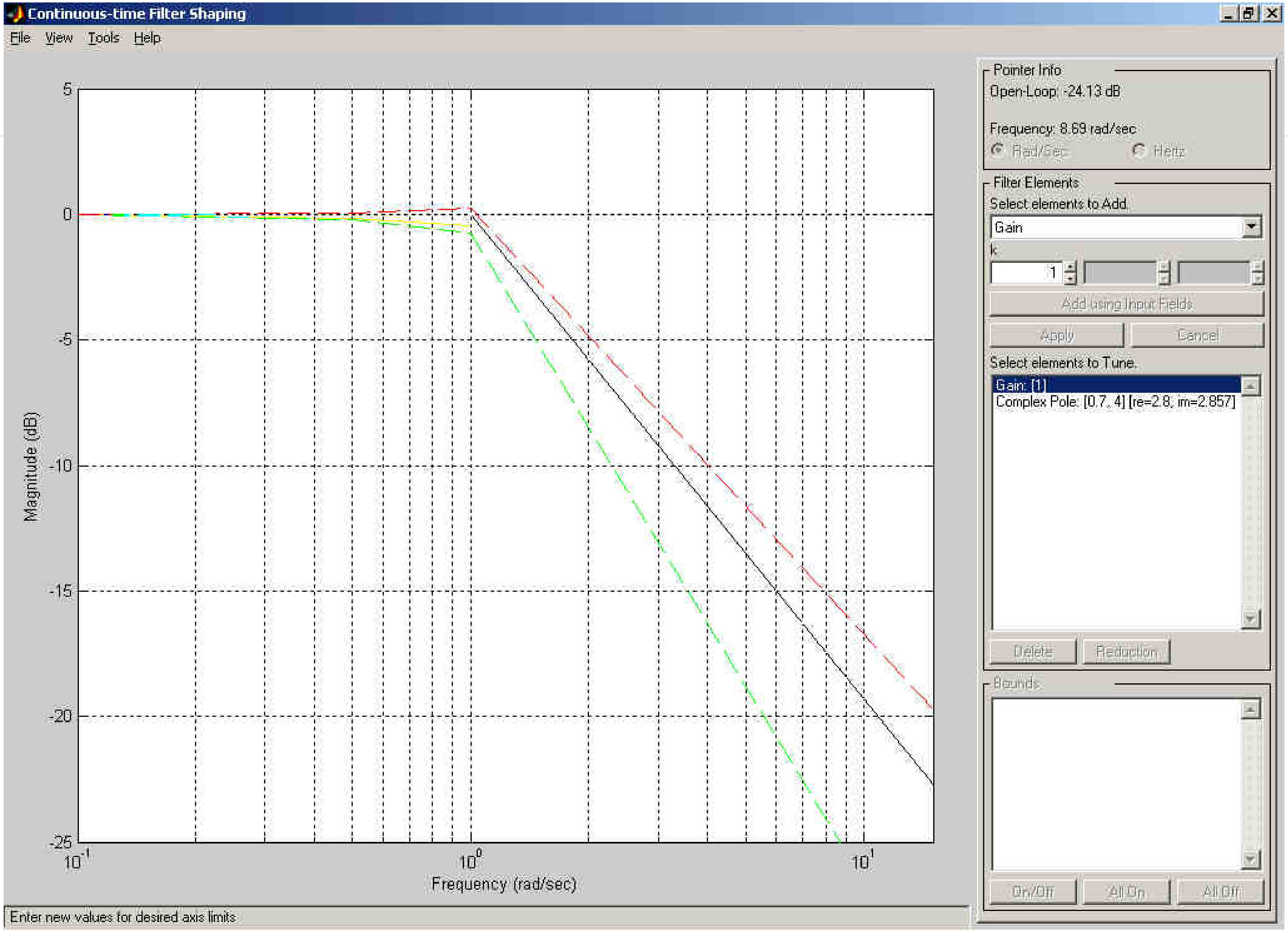

Step 12: Simulate linear system (J time responses)
Step 13: Simulate with nonlinearities

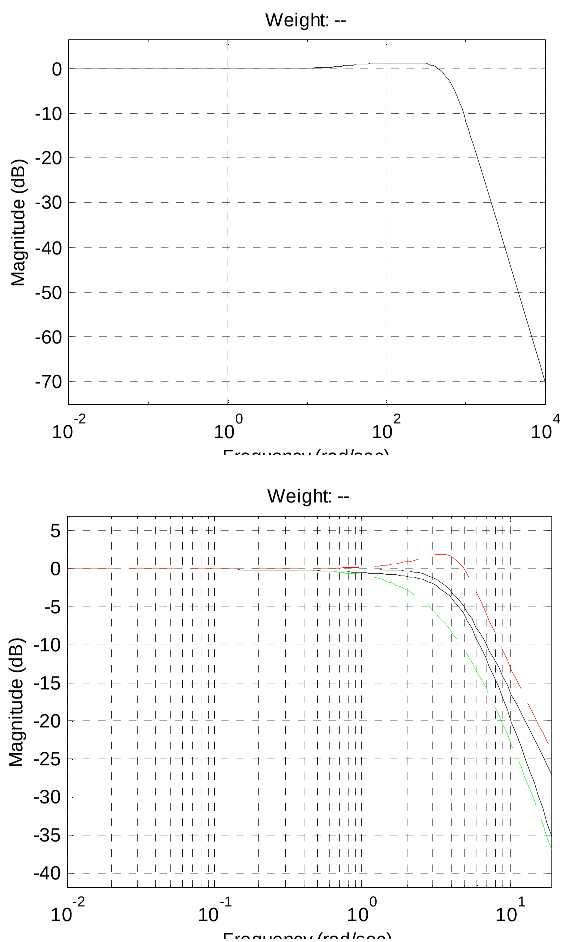

Frequency Domain

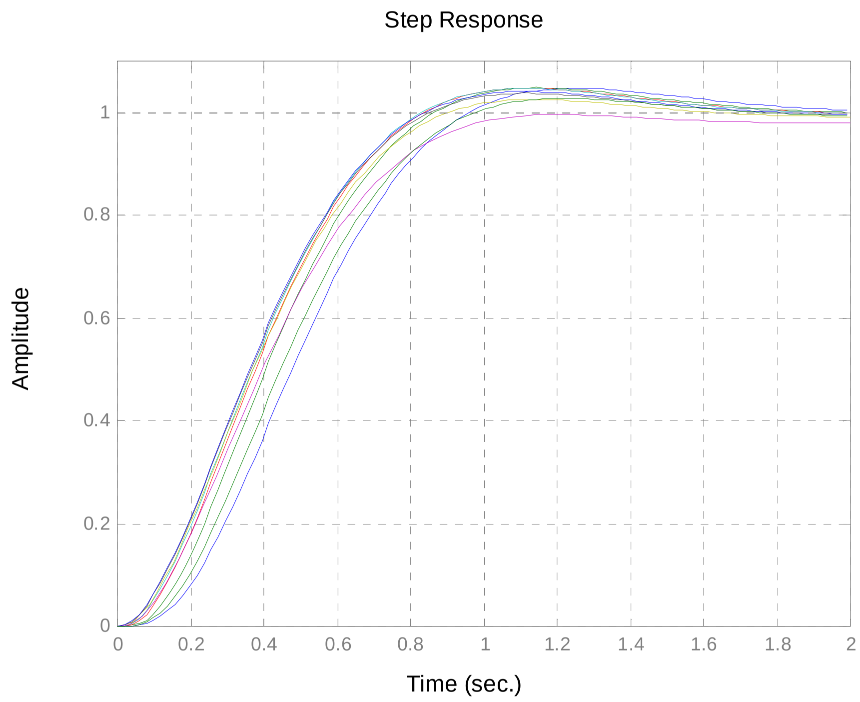

Time Domain

Mario Garcia-Sanz

Design procedure:

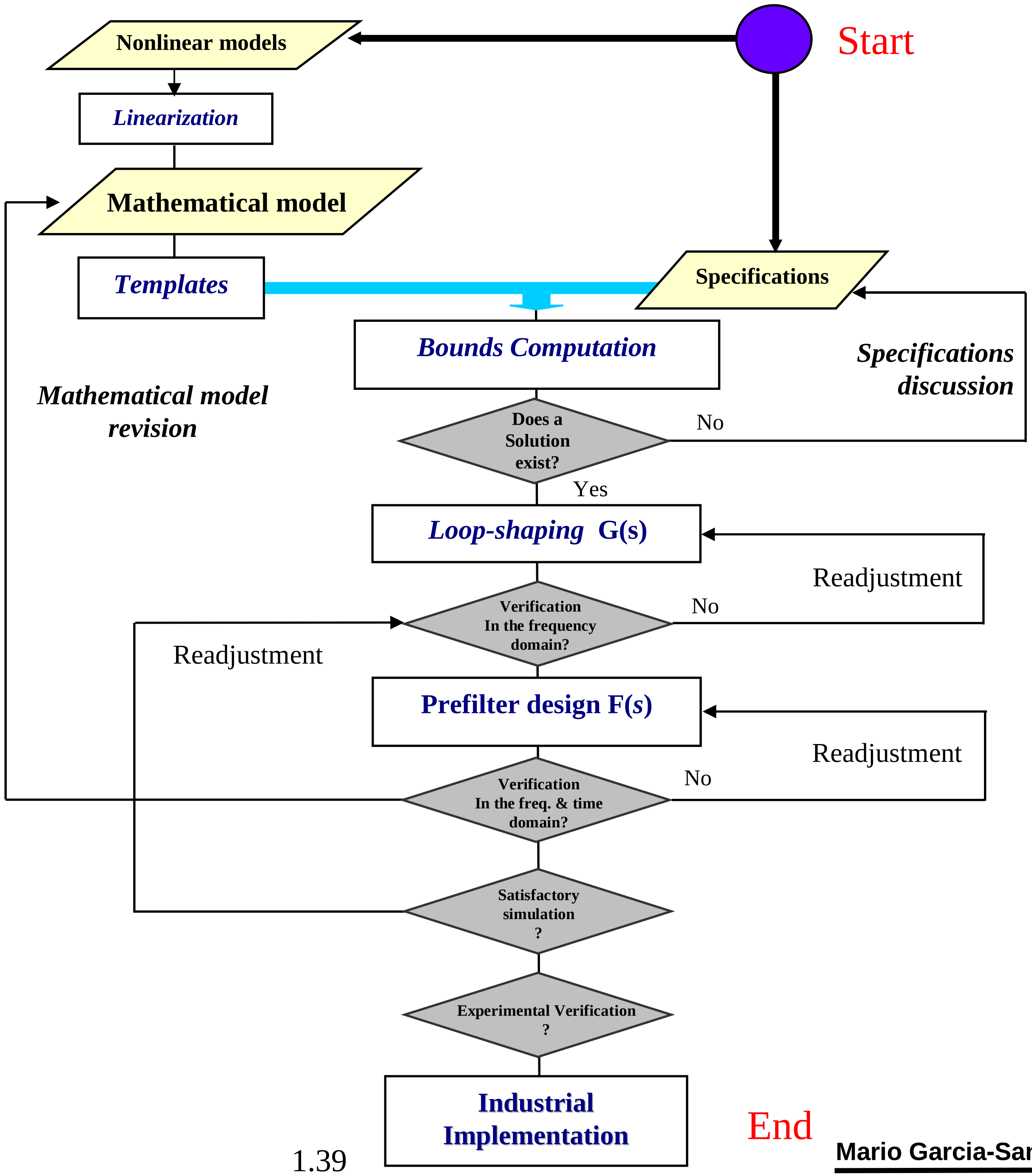

Mario Garcia-Sanz

1.3.- References

- Books:

  - **HOROWITZ, I. M.**, 1993, *Quantitative Feedback Design Theory (QFT).* QFT Pub., 660 South Monaco Parkway, Denver, Colorado 80224-1229.
  - **YANIV, O.**, 1999, *Quantitative Feedback Design of Linear and Non-linear Control Systems*. Kluver Academic Pub., ISBN: 0-7923-8529-2.
  - **SIDI, M.**., 2002, *Design of Robust Control Systems: From classical to modern practical approaches*. Krieger Publishing.
  - **HOUPIS, CH., RASMUSSEN, SJ., GARCIA-SANZ, M.,** 2006, *Quantitative Feedback Theory. Fundamentals and Applications.* 2nd Edition. A CRC book, Taylor and Francis.

- C.H. Houpis, S.J. Rasmussen and M. García-Sanz

  "Quantitative Feedback Theory. Fundamentals and applications". 2nd edition, 624 pages, a CRC Press book, ***Taylor & Francis***, Boca Ratón, Florida, USA, ISBN: 0849333709, January 2006.

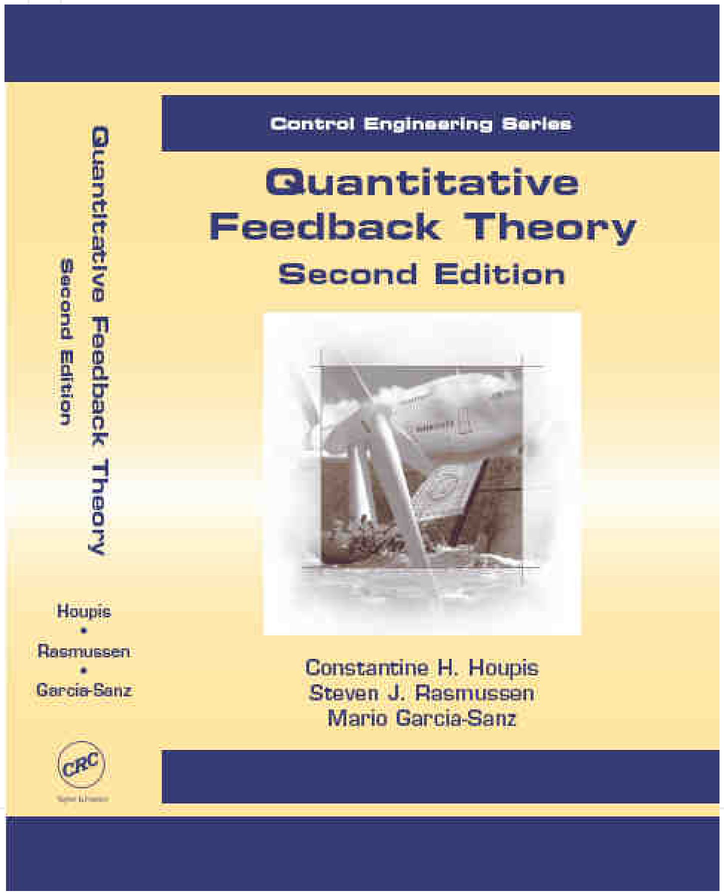

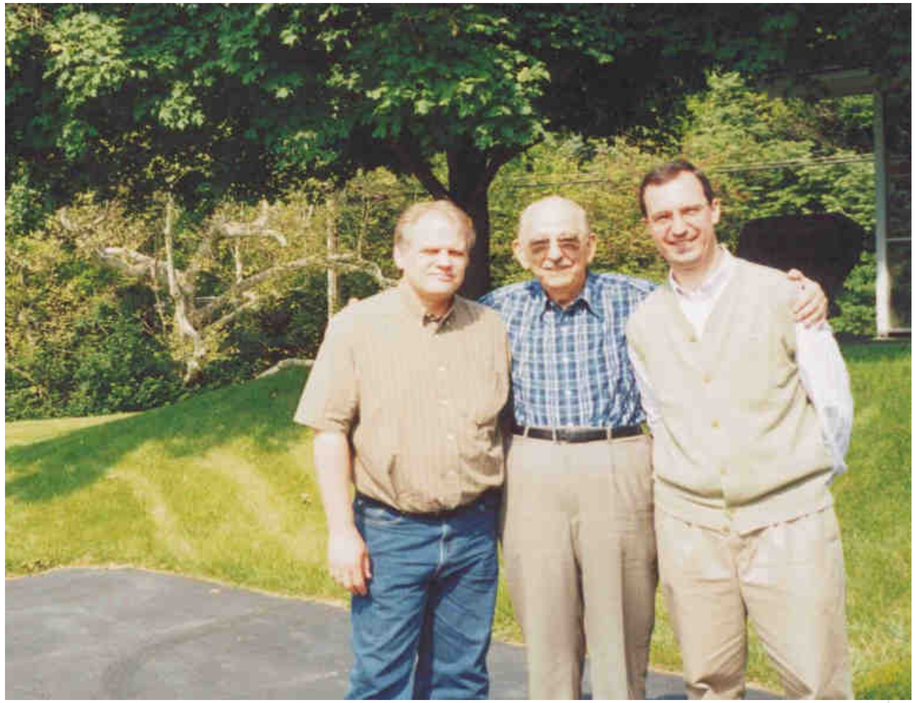

Air Force Institute of Technology
Wright-Patterson AFB,
Dayton, Ohio, USA, 2003

Taylor & Francis CRC Press

- C.H. Houpis, S.J. Rasmussen and M. García-Sanz

  "Solutions Manual to Quantitative Feedback Theory. Fundamentals and applications". 2nd edition, 90 pages, ***Taylor & Francis***, Boca Ratón, Florida, USA, January 2006.

- International Symposia on Quantitative Feedback Theory and Robust Frequency Domain Methods
  - Up to now there have been eight Int. Symp. on QFT:

1.- **Houpis, C.H., Chander, P**. (Editors). Writght Patterson Airforce Base, Dayton, Ohio, USA, August 1992.

2.- **Nwokah, O.D.I., Chander, P.** (Editors). Purdue University, West Lafayette, Indiana, USA, August 1995.

3.- **Petropoulakis, L., Leithead, W.E.**(Editors). University of Strathclyde, Glasgow, Scotland, UK, August 1997.

4.- **Boje, E., and Eitelberg, E.** (Editors). University of Natal, Durban, South Africa, August 1999.

5.- **García-Sanz, M.** (Editor). Public University of Navarra, Pamplona, Spain, August 2001.

6.- **Boje, E., and Eitelberg, E.** (Editors). University of Cape Town, Cape Town, South Africa, December 2003.

7.- **Colgren, R.** (Editor). University of Kansas, Lawrence, Kansas, USA, August 2005.

8.- **Gutman, P-O.** (Editor). Technion, Haifa, Israel, July 2007.

- Special Issues:

1.- Nwokah, O.D.I. (Guest Editor). **Horowitz and QFT Design Methods. Special Issue**. *International Journal of Robust and Nonlinear Control*. Vol. 4, Num 1, January-February 1994. Wiley.

2.- Houpis, C.H. (Guest Editor). **Quantitative Feedback Theory. Special Issue**. *International Journal of Robust and Nonlinear Control*. Vol. 7, Num 6, June 1997. Wiley.

3.- Eitelberg, Eduard (Guest Editor). **Isaac Horowitz. Special Issue**. *International Journal of Robust and Nonlinear Control*. Part 1, Vol. 11, Num 10, August 2001 and Part 2, Vol. 12, Num 4, April 2002. Wiley.

4.- Garcia-Sanz, Mario (Guest Editor). **Robust Frequency Domain. Special Issue**. *International Journal of Robust and Nonlinear Control*. Vol. 13, Num 7, June 2003. Wiley.

5.- Garcia-Sanz, Mario and Houpis, Constantine (Guest Editors). **Quantitative Feedback Theory. In Memoriam of Isaac Horowitz. Special Issue**. *International Journal of Robust and Nonlinear Control*. Vol. 17, Num 2-3, January 2007. Wiley.

1.4.- QFT Software tools

- **BORGHESANI, C., CHAIT, Y., YANIV, O.,** 2002,
  Quantitative Feedback Theory Toolbox - For use with MATLAB, 2nd Ed.
  USA
  http://www.terasoft.com/products/qft/

- **GUTMAN, P.O**.,
  Qsyn.
  Haifa, Israel.

- **HOUPIS, C.H., RASMUSSEN, S., GARCIA-SANZ, M**., 2006
  QFT CAD Tool for MISO and MIMO systems.
  With the book, *Quantitative Feedback Theory. Fundamentals and applications*
  Taylor and Francis, 2nd edition
  USA

Outline

1.- QFT Controller Design Technique Fundamentals

2.- Real-world QFT control applications and examples

3.- Non-diagonal MIMO QFT controller design methodologies

4.- Application: Robust QFT control for a MIMO Spacecraft with flexible sunshield

5.- Switching robust control: Beyond the linear limitations.

6.- Example: Switching control for Unmanned Vehicles

2.- Real-world QFT control applications: Control of a Large Wind Turbine

Multipole,
Variable Speed, Direct Drive
1650 kW Wind Turbine.
TWT1650. M.Torres (Spain).

TORRES WIND TURBINE, TWT 1650

- More than 20 control loops
- Very Non-linear models
- MIMO plant
- Parameter uncertainty
- High reliability needed
- Optimum efficiency

E. Torres, M. García-Sanz

"Experimental Results of the Variable Speed, Direct Drive Multipole Synchronous Wind Turbine: TWT1650". **Wind Energy**, 2004.

TWT1650.

Mechanical Diagram

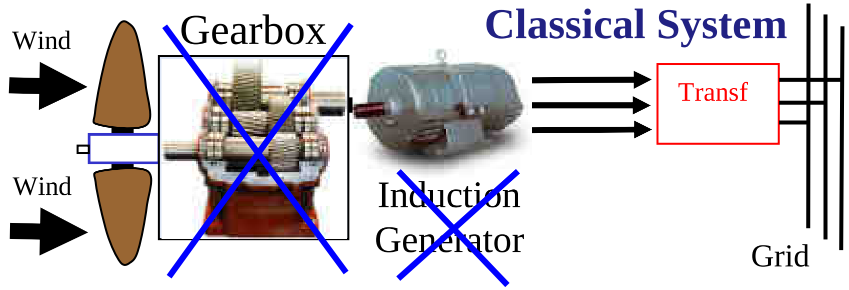

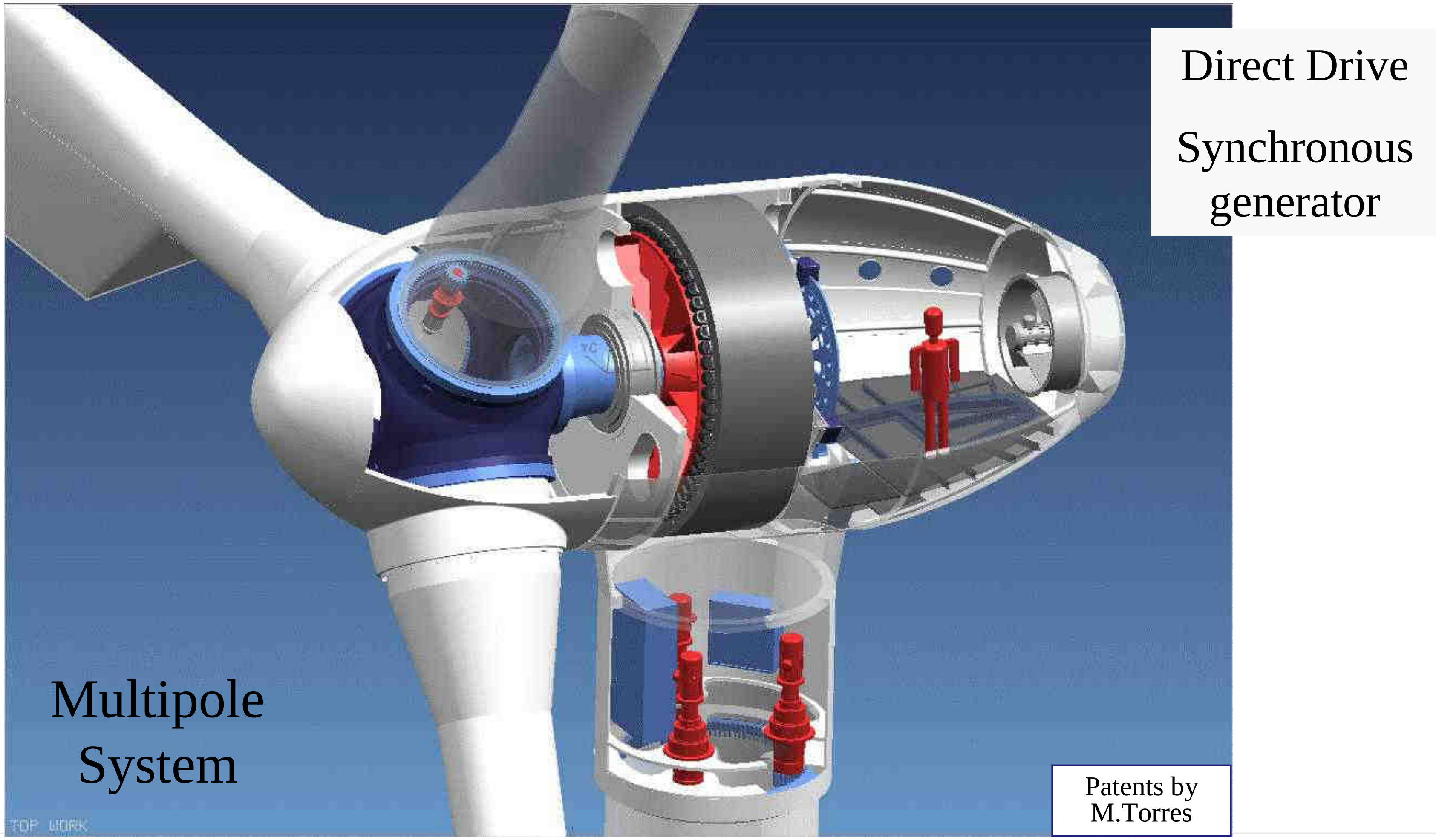

Mario Garcia-Sanz

TWT1650. Electrical Block Diagram

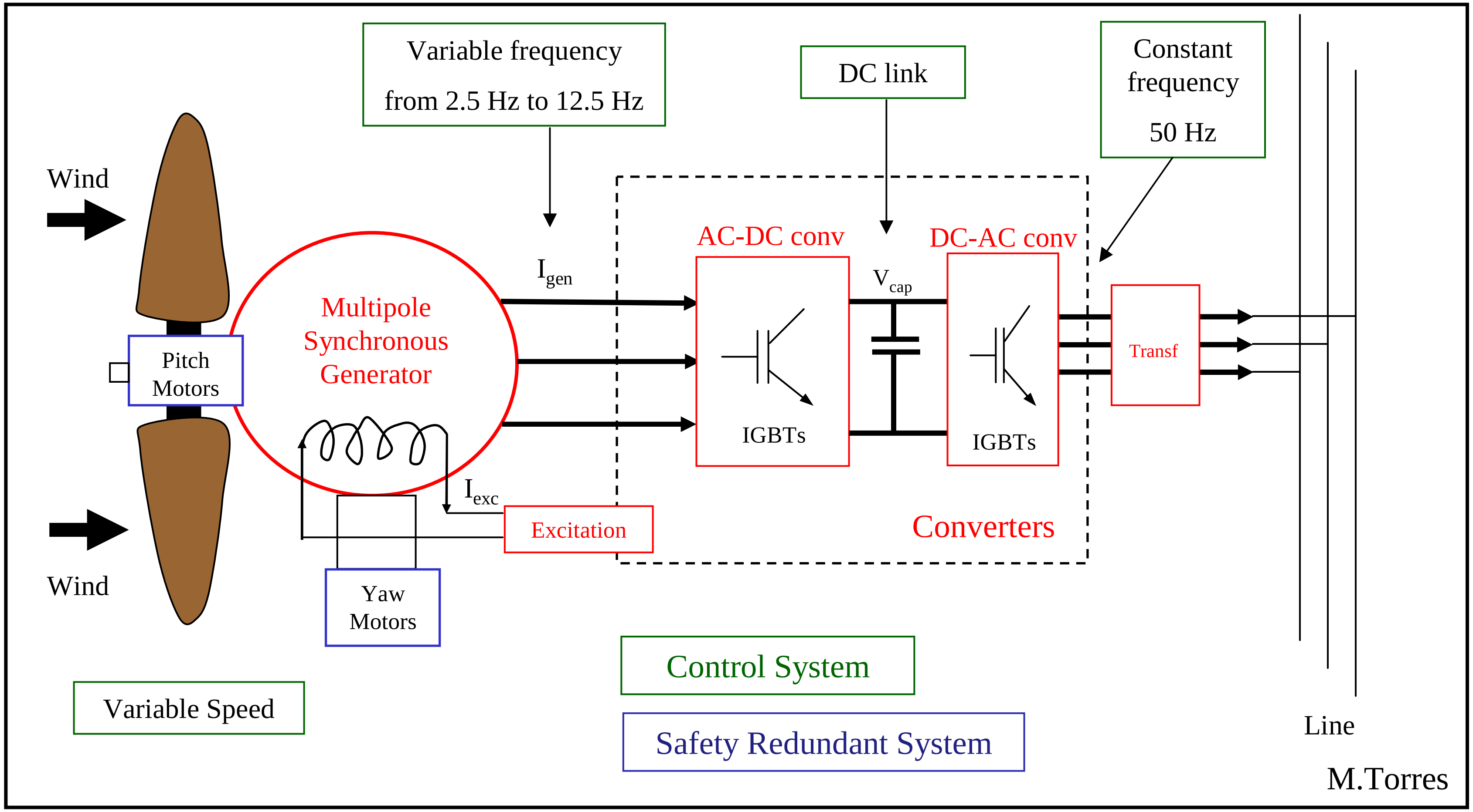

TWT-1650

TWT1650. First Prototype built in May 2001

M.Torres

First Prototype at Cabanillas Wind Farm (Spain)

TWT1650. First Prototype built in May 2001

M.Torres

Tower: 70 m ; Blade: 40 m
Rotor: 82 m ; Inertia rotor: 5,000,000 Kg m^2

TWT1650. Actual Results.

Example of three of more than 20 loops.

M.Torres

Target: To control the Wind Turbine Rotor Speed .
Actuators: Pitch angle movement. 3 Independent driven blades.

Control Loop 1:	Input:	Wind Turbine Rotor Speed Ref. = 20 rpm
	Output:	Pitch Angle Reference.
Control Loop 2:	Input:	Pitch Angle Reference.
	Output:	Pitch Speed Reference.
Control Loop 3:	Input	Pitch Speed Reference.
	Output:	Motor Current Reference.

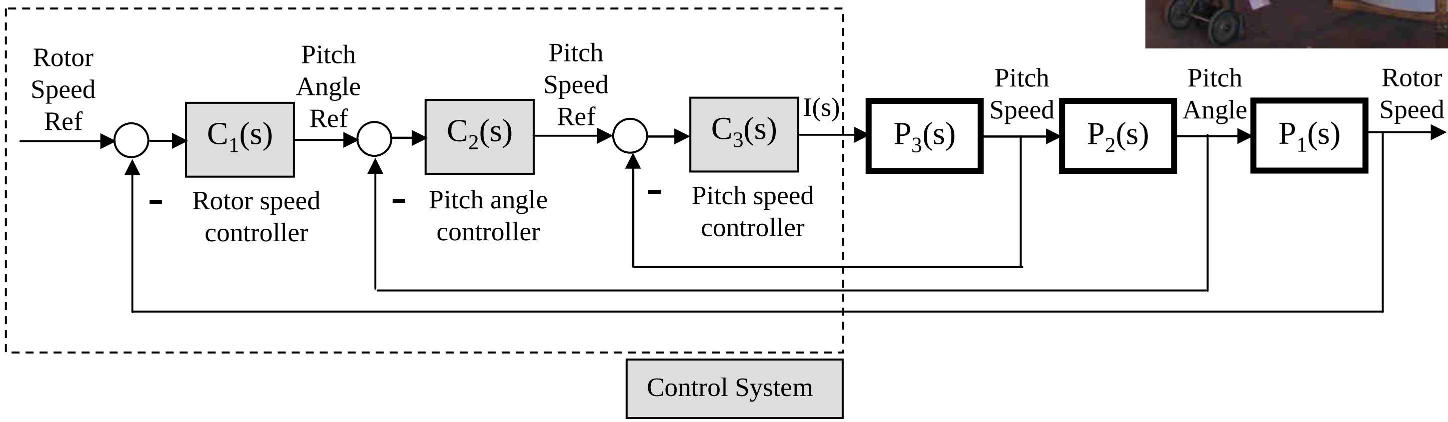

Mario Garcia-Sanz

TWT1650. Actual Results.

Example of three of more than 20 loops.

M.Torres

06.April.2003. Cabanillas Wind Farm (Spain).

Very High Wind: Aver. 24 m/s

Target: control Rotor Speed (r.p.m.).

Set-point: 20 rpm

Actuators: Pitch angle movement.

3 Independent driven blades.

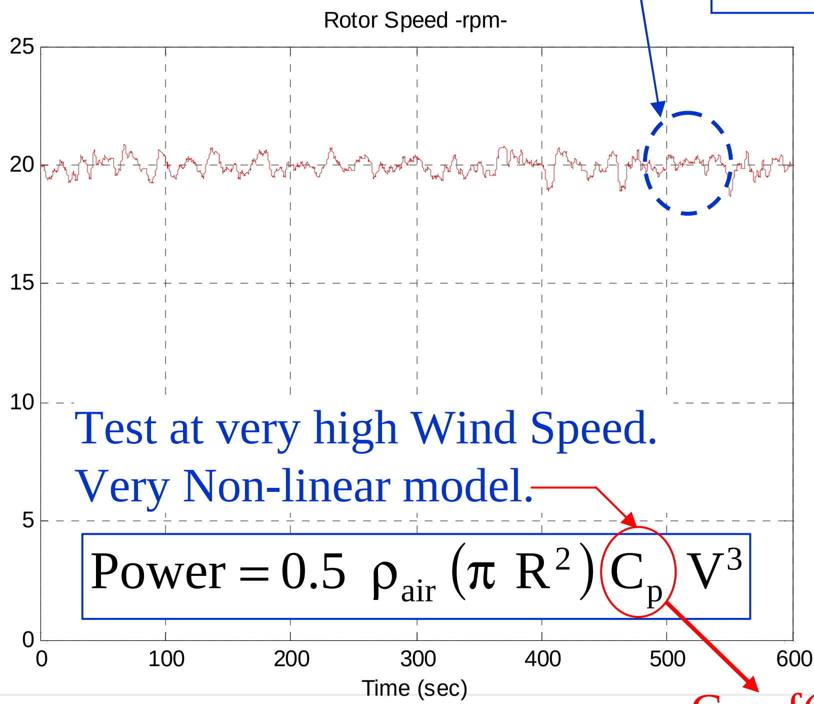

Test at very high Wind Speed.

Very Non-linear model.

$$\text{Power} = 0.5\ \rho_{air}\ (\pi\ R^2)\ C_p\ V^3$$

$C_p = f(V,\Omega,\beta)$

4.5 MW
2140 kNm

Wind Gust

1.7 MW
800 kNm

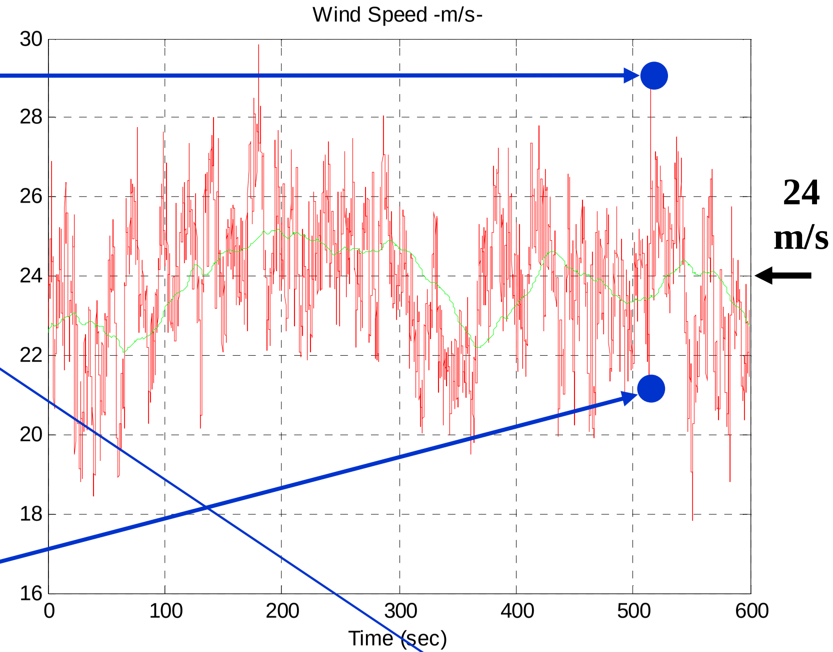

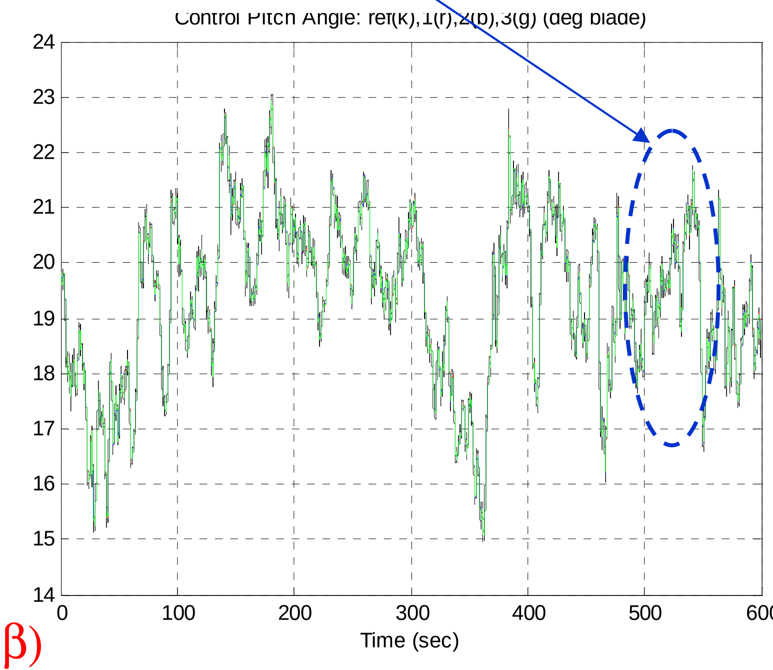

Mario Garcia-Sanz

TWT1650. Actual Results.

Example of three of more than 20 loops.

M.Torres

04.February.2003. Cabanillas Wind Farm (Spain).

<u>Medium Wind:</u> Average 15 m/s

<u>Target</u>: control Rotor Speed (r.p.m.).

<u>Set-point</u>: 20 rpm

<u>Actuators</u>: Pitch angle movement.

3 Independent driven blades.

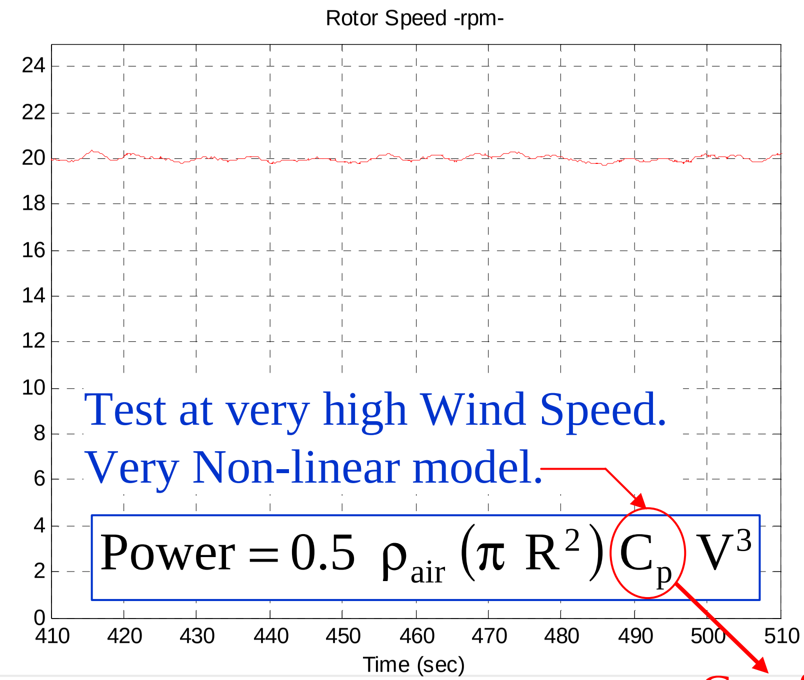

Test at very high Wind Speed.

Very Non-linear model.

$$\text{Power} = 0.5\ \rho_{air}\,(\pi\ R^2)\,C_p\ V^3$$

$$C_p = f(V,\Omega,\beta)$$

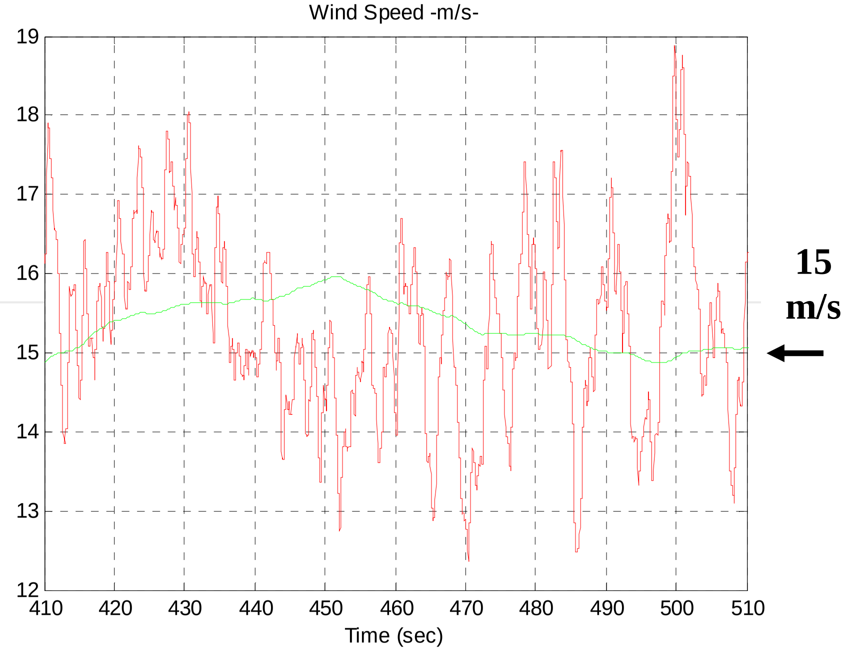

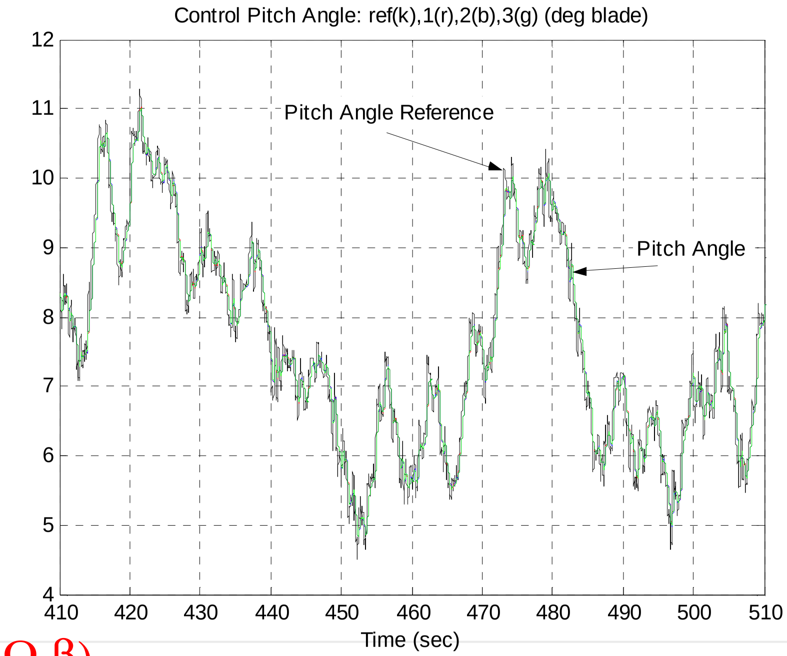

Mario Garcia-Sanz

Outline

1.- QFT Controller Design Technique Fundamentals

2.- Real-world QFT control applications and examples

3.- Non-diagonal MIMO QFT controller design methodologies

4.- Application: Robust QFT control for a MIMO Spacecraft with flexible sunshield

5.- Switching robust control: Beyond the linear limitations.

6.- Example: Switching control for Unmanned Vehicles

3. Non-diagonal MIMO QFT Controller Design Methodologies

This section discusses how the QFT technique can be applied to the design of MIMO control systems.

2x2 Example of a MIMO system (non-diagonal controller)

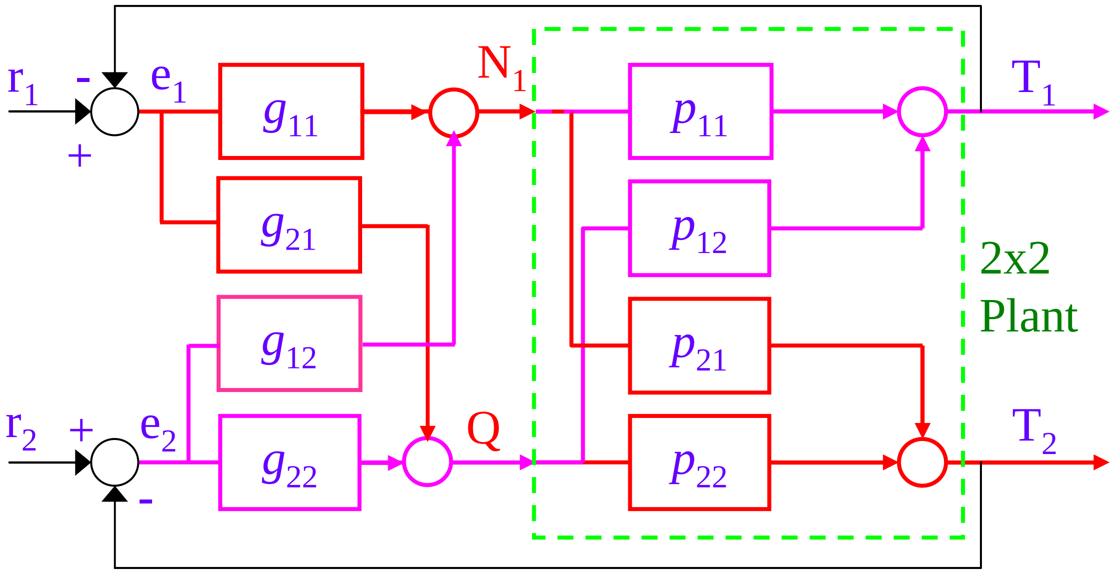

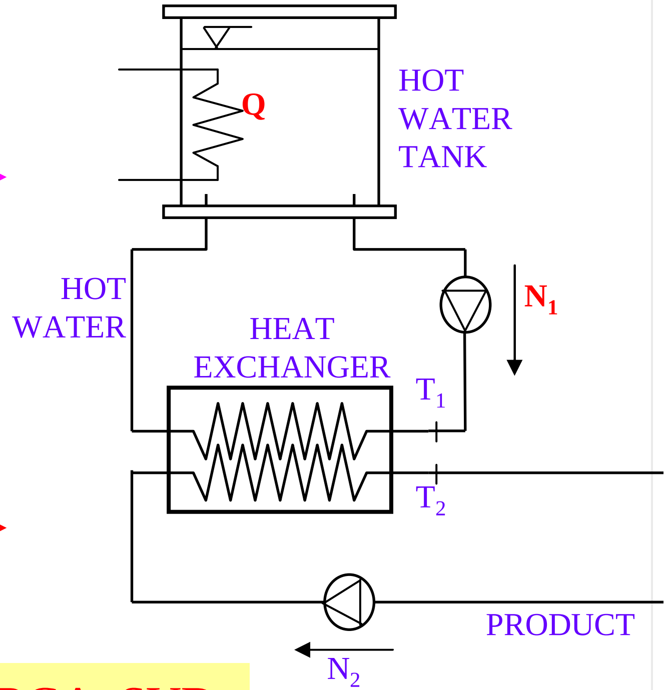

New Problems: Interaction between control loops, Input and output Directions, Input-output Pairing, Transmission Zeros (RHP).

New Tools: RGA, SVD, Smith-McMillan…

Mario Garcia-Sanz

3.1.- Introduction

García-Sanz M., Egaña I. (2002). **Quantitative Non-diagonal Controller Design for Multivariable Systems with Uncertainty**. *Int. J. Robust Nonlinear Control*, Vol. 12, No. 4, pp. 321-333.

García-Sanz M., Egaña I., Barreras M. (2005). **Design of quantitative feedback theory non-diagonal controllers for use in uncertain multiple-input multiple-output systems**. *IEE Control Theory and Applications*. Vol. 152, N. 02, pp. 177-187.

- A fully populated (non-diagonal) matrix compensator allows the designer much more design **flexibility** to govern MIMO systems than the classical diagonal controller.
- This session **extends** the classical diagonal QFT compensator design to a fully populated matrix compensator design.
- In this session **three cases** are studied:
  - ➔ - the reference tracking,
  - ➔ - the external disturbance rejection at the plant input and
  - ➔ - the external disturbance rejection at plant output.
- The definition of three **coupling matrices** (C_1, C_2, C_3) of the non-diagonal elements are used to quantify the amount of loop interaction and to design the non-diagonal compensators respectively.
- This yields a criterion to propose a **sequential design methodology** of the fully populated matrix compensator in the QFT robust control frame.

MIMO System

- Consider an *nxn* linear multivariable system (see Figure), composed of a plant ***P***, a fully populated matrix compensator ***G***, and a prefilter ***F***:

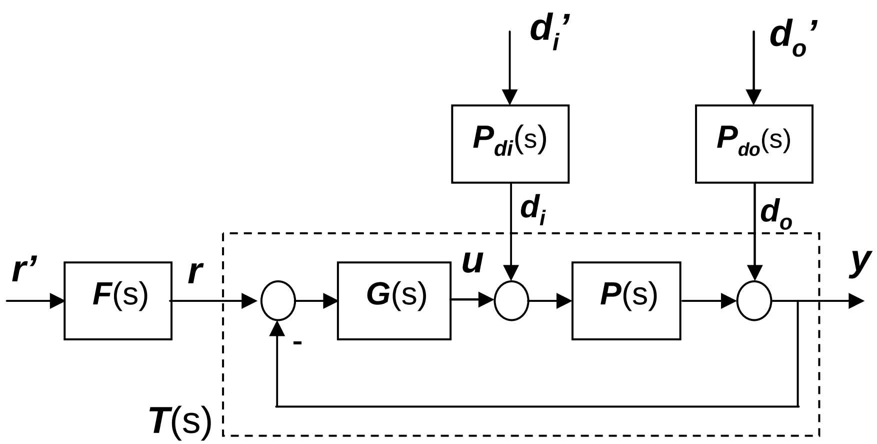

$$\mathbf{P} = \begin{bmatrix} p_{11} & p_{12} & \cdots & p_{1n} \\ p_{21} & p_{22} & \cdots & p_{2n} \\ \vdots & \vdots & \ddots & \vdots \\ p_{n1} & p_{n2} & \cdots & p_{nn} \end{bmatrix}; \quad \mathbf{G} = \begin{bmatrix} g_{11} & g_{12} & \cdots & g_{1n} \\ g_{21} & g_{22} & \cdots & g_{2n} \\ \vdots & \vdots & \ddots & \vdots \\ g_{n1} & g_{n2} & \cdots & g_{nn} \end{bmatrix};$$

$$\mathbf{F} = \begin{bmatrix} f_{11} & f_{12} & \cdots & f_{1n} \\ f_{21} & f_{22} & \cdots & f_{2n} \\ \vdots & \vdots & \ddots & \vdots \\ f_{n1} & f_{n2} & \cdots & f_{nn} \end{bmatrix}$$

where $P \in \mathcal{P}$, and $\mathcal{P}$ is the set of possible plants due to uncertainty.

- The plant inverse, denoted by $\boldsymbol{P}^*$, is presented in the following format:

$$\boldsymbol{P}^{-1} = \boldsymbol{P}^* = \left[p^*_{ij}\right] = \boldsymbol{\Lambda} + \boldsymbol{B} = \begin{bmatrix} p^*_{11} & 0 & 0 \\ 0 & \cdots & 0 \\ 0 & 0 & p^*_{nn} \end{bmatrix} + \begin{bmatrix} 0 & \dots & p^*_{1n} \\ \dots & 0 & \dots \\ p^*_{n1} & \dots & 0 \end{bmatrix}$$

- and where the compensator matrix is broken up into two parts as follows:

$$\boldsymbol{G} = \boldsymbol{G}_d + \boldsymbol{G}_b = \begin{bmatrix} g_{11} & 0 & 0 \\ 0 & \dots & 0 \\ 0 & 0 & g_{nn} \end{bmatrix} + \begin{bmatrix} 0 & \dots & g_{1n} \\ \dots & 0 & \dots \\ g_{n1} & \dots & 0 \end{bmatrix}$$

The following introduces a measurement index to quantify the loop interaction in the three classical cases: reference tracking, external disturbances at the plant input, and the external disturbances at the plant output.

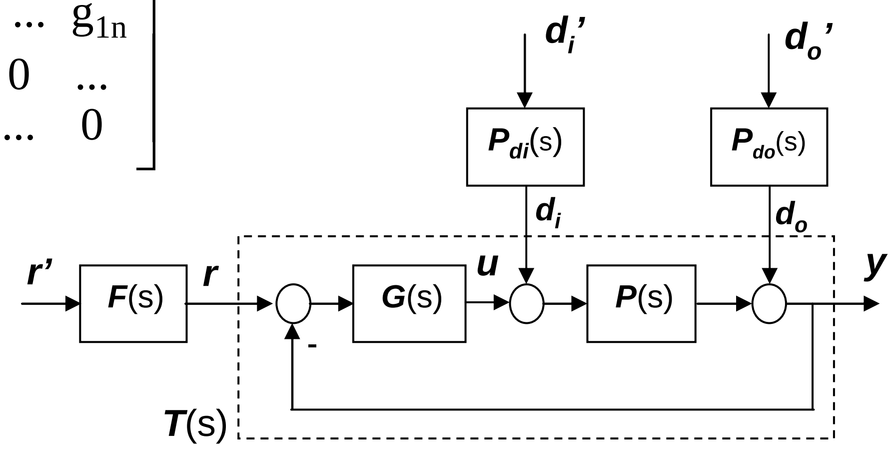

Mario Garcia-Sanz

Reference Tracking.

- The transfer function matrix of the control system for the reference tracking problem, without any external disturbance, is written as follows:

$$y = (I + P\ G)^{-1}\ P\ G\ r = T_{y/r}\ r = T_{y/r}\ F\ r'$$

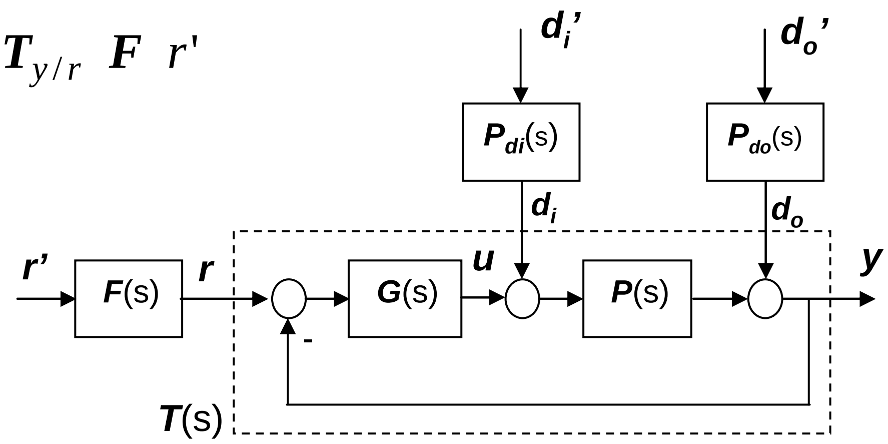

and applying the definitions of :

$P^* = \Lambda + B$ and $G = G_d + G_b$

$$T_{y/r}\ r = \boxed{(I + \Lambda^{-1}\ G_d)^{-1}\ \Lambda^{-1}\ G_d\ r} + \boxed{(I + \Lambda^{-1}\ G_d)^{-1}\ \Lambda^{-1}\left[G_b\ r - (B + G_b)\ T_{y/r}\ r\right]}$$

A diagonal term

A non-diagonal term

Mario Garcia-Sanz

- A diagonal term: $\boldsymbol{T}_{y/r\_d} = \boxed{\left(\boldsymbol{I} + \boldsymbol{\Lambda}^{-1}\ \boldsymbol{G}_d\right)^{-1}\ \boldsymbol{\Lambda}^{-1}\ \boldsymbol{G}_d}$

A diagonal term

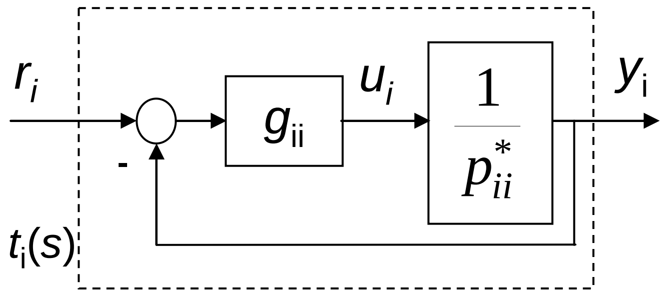

- A non-diagonal term: $\boldsymbol{T}_{y/r\_b} = \boxed{\left(\boldsymbol{I} + \boldsymbol{\Lambda}^{-1}\ \boldsymbol{G}_d\right)^{-1}\ \boldsymbol{\Lambda}^{-1}\ \left[\boldsymbol{G}_b - \left(\mathbf{B} + \boldsymbol{G}_b\right)\ \boldsymbol{T}_{y/r}\right]} = \left(\boldsymbol{I} + \boldsymbol{\Lambda}^{-1}\ \boldsymbol{G}_d\right)^{-1}\ \boldsymbol{\Lambda}^{-1}\ \boldsymbol{C}_1$

A non-diagonal term

$d_j = \sum_{k=1}^{n} c_{1ij}\, r_j$

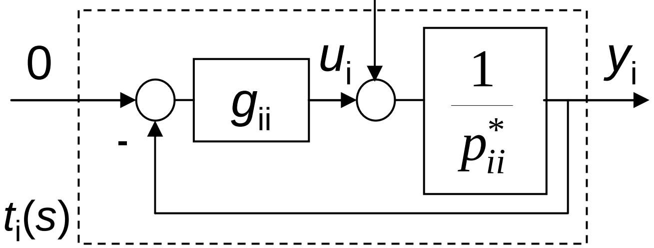

$$\boldsymbol{C}_1 = \boldsymbol{G}_b - \left(\boldsymbol{B} + \boldsymbol{G}_b\right)\boldsymbol{T}_{y/r} = \begin{bmatrix} c_{1_{11}} & c_{1_{12}} & \cdots & c_{1_{1m}} \\ c_{1_{21}} & c_{1_{22}} & \cdots & c_{1_{2m}} \\ \vdots & \vdots & \ddots & \vdots \\ c_{1_{m1}} & c_{1_{m2}} & \cdots & c_{1_{mm}} \end{bmatrix}$$

$$c_{1ij} = g_{ij}\left(1 - \delta_{ij}\right) - \sum_{k=1}^{n}\left(p^*_{ik} + g_{ik}\right) t_{kj}\left(1 - \delta_{ik}\right)$$

$$\delta_{ki} = \begin{cases} \delta_{ki} = 1 \Leftrightarrow k = i \\ \delta_{ki} = 0 \Leftrightarrow k \neq i \end{cases}$$

C_1 represents the *coupling matrix C* of the equivalent system for reference tracking problems

External disturbance rejection at plant input.

- The transfer function matrix of the control system for the external disturbance rejection at plant input problem, without any external disturbance, is written as,

$$y = \left(\boldsymbol{I} + \boldsymbol{P}\ \boldsymbol{G}\right)^{-1} \boldsymbol{P}\, d_i = \boldsymbol{T}_{y/di}\, d_i = \boldsymbol{T}_{y/di}\, P_{di}\ d_i'$$

and applying the definitions of $\boldsymbol{P}^* = \boldsymbol{\Lambda} + \boldsymbol{B}$ and $\boldsymbol{G} = \boldsymbol{G}_{\mathrm{d}} + \boldsymbol{G}_{\mathrm{b}}$

$$\boldsymbol{T}_{y/di}\, \mathrm{d}_i = \boxed{\left(\boldsymbol{I} + \boldsymbol{\Lambda}^{-1} \boldsymbol{G}_{\mathrm{d}}\right)^{-1} \boldsymbol{\Lambda}^{-1}\, \mathrm{d}_i} - \boxed{\left(\boldsymbol{I} + \boldsymbol{\Lambda}^{-1} \boldsymbol{G}_{\mathrm{d}}\right)^{-1} \boldsymbol{\Lambda}^{-1} \left[\left(\mathbf{B} + \boldsymbol{G}_{\mathrm{b}}\right) \boldsymbol{T}_{\mathrm{y/di}}\right] \mathrm{d}_i}$$

A diagonal term

A non-diagonal term

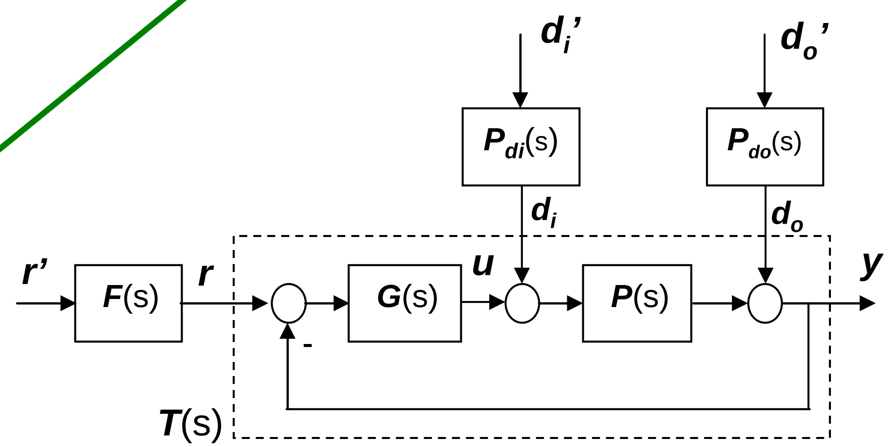

Mario Garcia-Sanz

- A diagonal term: $\boldsymbol{T}_{y/di\_d} = \boxed{\left(\boldsymbol{I} + \boldsymbol{\Lambda}^{-1}\boldsymbol{G}_d\right)^{-1}\boldsymbol{\Lambda}^{-1}}$

A diagonal term

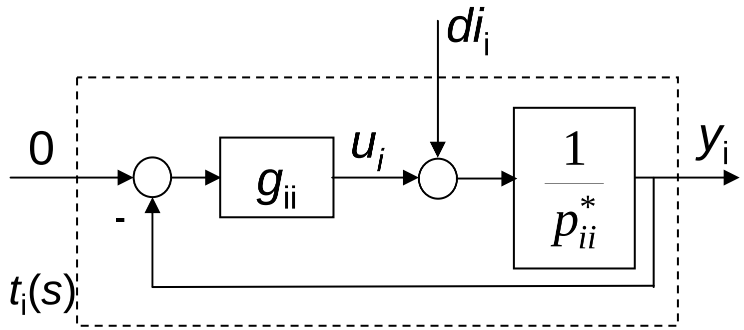

- A non-diagonal term:

$$\boldsymbol{T}_{y/di\_b} = \boxed{\left(\boldsymbol{I} + \Lambda^{-1}\boldsymbol{G}_d\right)^{-1}\Lambda^{-1}\left(\mathrm{B} + \boldsymbol{G}_b\right)\boldsymbol{T}_{y/di}} = \left(\boldsymbol{I} + \Lambda^{-1}\boldsymbol{G}_d\right)^{-1}\Lambda^{-1}\boldsymbol{C}_2$$

A non-diagonal term

$$d_j = \sum_{k=1}^{n} c_{2ij}\, di_j$$

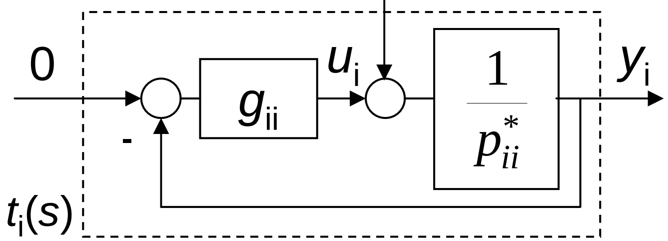

$$\boldsymbol{C}_2 = \left(\mathbf{B} + \boldsymbol{G}_b\right)\boldsymbol{T}_{y/di}$$

$$c_{2ij} = \sum_{k=1}^{n}(p^*_{ik} + g_{ik})\, t_{kj}\,(1 - \delta_{ik})$$

$$\delta_{ki} = \begin{cases} \delta_{ki} = 1 \Leftrightarrow k = i \\ \delta_{ki} = 0 \Leftrightarrow k \neq i \end{cases}$$

C_2 represents the *coupling matrix* of the equivalent system for external disturbance rejection at the plant input problems

External disturbance rejection at plant output.

- The transfer function matrix of the control system for the external disturbance rejection at plant output problem, without any external disturbance, is written as,

$$y = (\boldsymbol{I} + \boldsymbol{P}\,\boldsymbol{G})^{-1}\, d_o = \boldsymbol{T}_{y/do}\, d_o = \boldsymbol{T}_{y/do}\, \mathbf{P}_{do}\, d_o'$$

and applying the definitions of $\boldsymbol{P}^* = \boldsymbol{\Lambda} + \boldsymbol{B}$ and $\boldsymbol{G} = \boldsymbol{G}_{\mathrm{d}} + \boldsymbol{G}_{\mathrm{b}}$

$$\boldsymbol{T}_{y/do}\, d_o = \boxed{\left(\boldsymbol{I} + \boldsymbol{\Lambda}^{-1}\boldsymbol{G}_{\mathrm{d}}\right)^{-1} d_o} + \boxed{\left(\boldsymbol{I} + \boldsymbol{\Lambda}^{-1}\boldsymbol{G}_{\mathrm{d}}\right)^{-1} \boldsymbol{\Lambda}^{-1}\left[\mathbf{B} - \left(\mathbf{B} + \boldsymbol{G}_{\mathrm{b}}\right)\boldsymbol{T}_{y/do}\right] d_o}$$

A diagonal term

A non-diagonal term

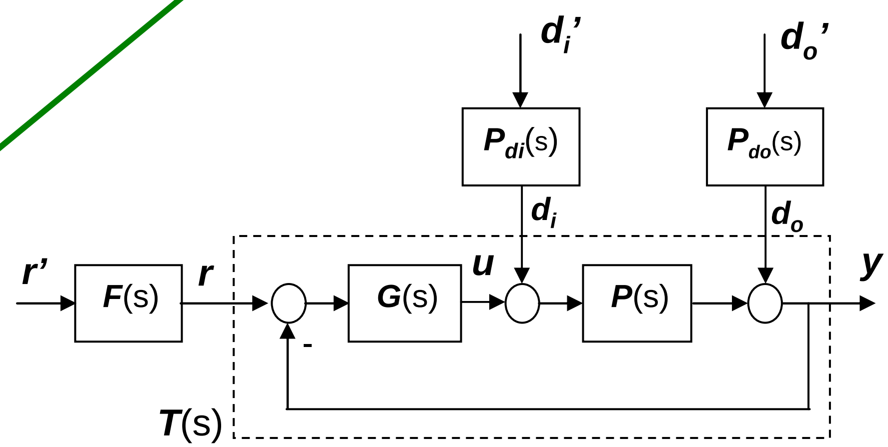

Mario Garcia-Sanz

- A diagonal term: $\boldsymbol{T}_{\mathrm{y/do\_d}} = \boxed{\left(\boldsymbol{I} + \boldsymbol{\Lambda}^{-1}\boldsymbol{G}_{\mathrm{d}}\right)^{-1}}$

A diagonal term

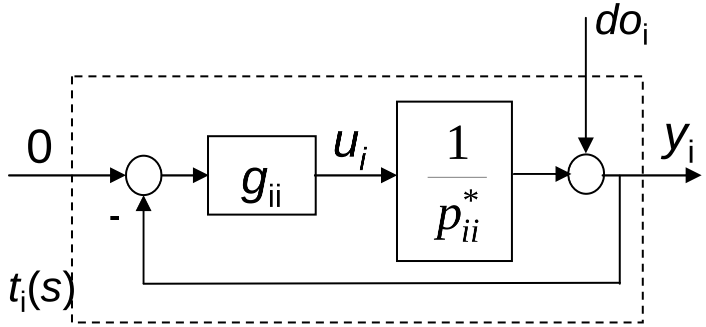

- A non-diagonal term: $\boldsymbol{T}_{\mathrm{y/do\_b}} = \boxed{\left(\boldsymbol{I} + \boldsymbol{\Lambda}^{-1}\boldsymbol{G}_{\mathrm{d}}\right)^{-1}\boldsymbol{\Lambda}^{-1}\left[\mathbf{B} - \left(\mathbf{B} + \boldsymbol{G}_{\mathrm{b}}\right)\boldsymbol{T}_{y/do}\right]} = \left(\boldsymbol{I} + \boldsymbol{\Lambda}^{-1}\boldsymbol{G}_{\mathrm{d}}\right)^{-1}\boldsymbol{\Lambda}^{-1}\boldsymbol{C}_3$

A non-diagonal term

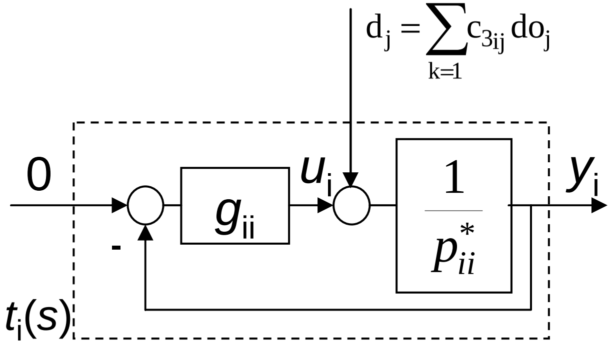

$$\boldsymbol{C}_3 = \boldsymbol{B} - \left(\boldsymbol{B} + \boldsymbol{G}_b\right)\boldsymbol{T}_{y/do}$$

$$c_{3ij} = p_{ij}^{*}\,(1-\delta_{ij}) - \sum_{k=1}^{n}(p_{ik}^{*} + g_{ik})\, t_{kj}\,(1-\delta_{ik})$$

$$\delta_{ki} = \begin{cases} \delta_{ki} = 1 \Leftrightarrow k = i \\ \delta_{ki} = 0 \Leftrightarrow k \neq i \end{cases}$$

C_3 represents the *coupling matrix* of the equivalent system for external disturbance rejection at the plant output problems

Mario Garcia-Sanz

The Coupling elements

- To design a MIMO compensator with a low coupling level, it is necessary to study the influence of every non-diagonal element g_{ij} on the coupling elements c_{1ij}, c_{2ij} and c_{3ij}.

- <u>Hypothesis</u>

$$\left|\left(p^*_{ij}+g_{ij}\right)\, t_{jj}\right| >> \left|\left(p^*_{ik}+g_{ik}\right) t_{kj}\right|, \text{ for } k \neq j, \text{ and in the bandwidth of } t_{jj}$$

- Thus,

$$\left|t_{jj}\right| >> \left|t_{kj}\right|, \text{ for } k \neq j, \text{ and in the bandwidth of } t_{jj}$$

- Due to hypothesis, the coupling effects c_{1ij}, c_{2ij}, c_{3ij} are computed as ,

$$c_{1ij} = g_{ij} - \frac{g_{jj}\left(p^*_{ij} + g_{ij}\right)}{\left(p^*_{jj} + g_{jj}\right)} \quad ; \quad i \neq j \qquad \text{tracking}$$

$$c_{2ij} = \frac{\left(p^*_{ij} + g_{ij}\right)}{\left(p^*_{jj} + g_{jj}\right)} \quad ; \quad i \neq j \qquad \text{disturbance rejection at the plant input}$$

$$c_{3ij} = p^*_{ij} - \frac{p^*_{jj}\left(p^*_{ij} + g_{ij}\right)}{\left(p^*_{jj} + g_{jj}\right)} \quad ; \quad i \neq j \qquad \text{disturbance rejection at plant output}$$

The Optimum non-diagonal controller

- The optimum non-diagonal compensators for the three cases (tracking and disturbance rejection at plant input and output) are obtained making last three Eqs. equal to zero.

$$g_{ij}^{opt} = F_{pd}\left(g_{jj} \frac{{p_{ij}^{*}}^{N}}{{p_{jj}^{*}}^{N}} \right), \text{ for } i \neq j \qquad \text{tracking}$$

$$g_{ij}^{opt} = F_{pd}\left(-{p_{ij}^{*}}^{N} \right), \text{ for } i \neq j \qquad \text{disturbance rejection at the plant input}$$

$$g_{ij}^{opt} = F_{pd}\left(g_{jj} \frac{{p_{ij}^{*}}^{N}}{{p_{jj}^{*}}^{N}} \right), \text{ for } i \neq j \qquad \text{disturbance rejection at plant output}$$

- where the function $F_{pd}(A)$ means in every case a stable proper function made from the dominant poles and zeros of the expression A.

Mario Garcia-Sanz

- Every uncertain plant can be any plant represented by the family:

$$\{p^*_{ij}\} = p^{*\,N}_{ij}\left(1+\Delta_{ij}\right) \quad , \quad 0 \le \left|\Delta_{ij}\right| \le \Delta\, p^*_{ij} \quad , \quad \text{for } i, j = 1,\ldots, n$$

- where $p^{*\,N}_{ij}$ is the nominal plant ($\neq P_o$), and Δp^*_{ij} is the maximum of the non-parametric uncertainty radii $\left|\Delta_{ij}\right|$

The nominal plants $p^{*\,N}_{ij}$ minimise the maximum of the non-parametric uncertainty radii Δp^*_{ij} and Δp^*_{jj} that comprise the plant templates.

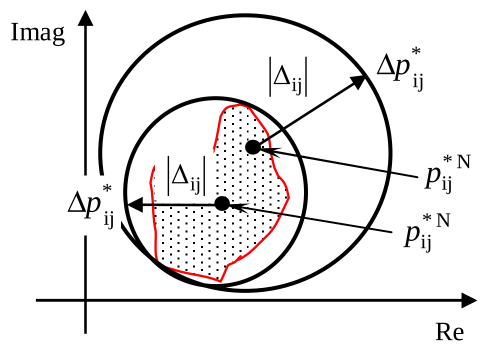

Design Methodology

$$G = \begin{bmatrix} g_{11} & 0 & \cdots & 0 & \cdots & 0 \\ g_{21} & 0 & \cdots & 0 & \cdots & 0 \\ \cdots & & \cdots & & \cdots & \\ g_{k1} & 0 & \cdots & 0 & \cdots & 0 \\ \cdots & & \cdots & & \cdots & \\ g_{n1} & 0 & \cdots & 0 & \cdots & 0 \end{bmatrix} \Rightarrow \begin{bmatrix} g_{11} & g_{12} & \cdots & 0 & \cdots & 0 \\ g_{21} & g_{22} & \cdots & 0 & \cdots & 0 \\ \cdots & & \cdots & & \cdots & \\ g_{k1} & g_{k2} & \cdots & 0 & \cdots & 0 \\ \cdots & & \cdots & & \cdots & \\ g_{n1} & g_{n2} & \cdots & 0 & \cdots & 0 \end{bmatrix} \Rightarrow \cdots$$

Step 1 Step 2

$$\cdots \Rightarrow \begin{bmatrix} g_{11} & g_{12} & \cdots & g_{1k} & \cdots & g_{1n} \\ g_{21} & g_{22} & \cdots & g_{2k} & \cdots & g_{2n} \\ \cdots & & \cdots & & \cdots & \\ g_{k1} & g_{k2} & \cdots & g_{kk} & \cdots & g_{kn} \\ \cdots & & \cdots & & \cdots & \\ g_{n1} & g_{n2} & \cdots & g_{nk} & \cdots & g_{nn} \end{bmatrix}$$

Step n

- **<u>Step A.</u>** *Controller Structure, Coupling Analysis, Input/output Pairing and loop ordering.*

  First, the methodology begins **pairing** the plant inputs and outputs and selecting the **controller structure** with the Relative Gain Analysis (RGA-Bristol) technique.

  This is followed by **arranging** the matrix ***P**** so that $(p^*_{11})^{-1}$ has the smallest phase margin frequency, $(p^*_{22})^{-1}$ the next smallest phase margin frequency, and so on.

  The **sequential** technique, composed of *n* stages (*n* loops), repeats steps (B and C) for every column k = 1 to n.

The compensator design method is a sequential procedure by closing loops.

Mario Garcia-Sanz

- **<u>Step B.</u>** *Design of the diagonal compensator elements g_{kk}.*

  This design of the element $g_{\underline{kk}}$ is calculated using the standard QFT loop-shaping technique for the inverse of the equivalent plant $\left(p^{*e}_{kk}\right)_k^{-1}$ in order to achieve robust stability and robust performance specifications.

$$\left[p^{*e}_{ik}\right]_i = \left[p^{*e}_{ik}\right]_{i-1} - \frac{\left(\left[p^{*e}_{i,i-1}\right]_{i-1} + g_{i,i-1}\right)\left(\left[p^{*e}_{i-1,k}\right]_{i-1} + g_{i-1,k}\right)}{\left(\left[p^{*e}_{i-1,i-1}\right]_{i-1} + g_{i-1,i-1}\right)}$$

$$\left[p^{*e}_{ik}\right]_1 = P^{-1}$$

$$\mathbf{G} = \begin{bmatrix} g_{11} & 0 & \dots & 0 & \dots & 0 \\ g_{21} & 0 & \dots & 0 & \dots & 0 \\ \dots & & \dots & & \dots & \\ g_{k1} & 0 & \dots & 0 & \dots & 0 \\ \dots & & \dots & & \dots & \\ g_{n1} & 0 & \dots & 0 & \dots & 0 \end{bmatrix} \Rightarrow \begin{bmatrix} g_{11} & g_{12} & \dots & 0 & \dots & 0 \\ g_{21} & g_{22} & \dots & 0 & \dots & 0 \\ \dots & & \dots & & \dots & \\ g_{k1} & g_{k2} & \dots & 0 & \dots & 0 \\ \dots & & \dots & & \dots & \\ g_{n1} & g_{n2} & \dots & 0 & \dots & 0 \end{bmatrix} \Rightarrow \dots$$

Step 1 Step 2

$$\dots \Rightarrow \begin{bmatrix} g_{11} & g_{12} & \dots & g_{1k} & \dots & g_{1n} \\ g_{21} & g_{22} & \dots & g_{2k} & \dots & g_{2n} \\ \dots & & \dots & & \dots & \\ g_{k1} & g_{k2} & \dots & g_{kk} & \dots & g_{kn} \\ \dots & & \dots & & \dots & \\ g_{n1} & g_{n2} & \dots & g_{nk} & \dots & g_{nn} \end{bmatrix}$$

Step n

$$\begin{bmatrix} p^*_{11}\big|_1 & p^*_{12}\big|_1 & p^*_{13}\big|_1 & \cdots & \cdots \\ p^*_{21}\big|_1 & p^*_{22}\big|_1 & p^*_{23}\big|_1 & \cdots & \cdots \\ p^*_{31}\big|_1 & p^*_{32}\big|_1 & p^*_{33}\big|_1 & \cdots & \cdots \\ \cdots & \cdots & \cdots & \cdots & \cdots \\ p^*_{k1}\big|_1 & p^*_{k2}\big|_1 & \cdots & p^{*e}_{kk}\big|_k & \cdots \end{bmatrix}$$

function of

Mario Garcia-Sanz

$$\mathbf{G} = \begin{bmatrix} g_{11} & 0 & \cdots & 0 & \cdots & 0 \\ g_{21} & 0 & \cdots & 0 & \cdots & 0 \\ \cdots & & \cdots & & \cdots & \\ g_{k1} & 0 & \cdots & 0 & \cdots & 0 \\ \cdots & & \cdots & & \cdots & \\ g_{n1} & 0 & \cdots & 0 & \cdots & 0 \end{bmatrix} \Rightarrow \begin{bmatrix} g_{11} & g_{12} & \cdots & 0 & \cdots & 0 \\ g_{21} & g_{22} & \cdots & 0 & \cdots & 0 \\ \cdots & & \cdots & & \cdots & \\ g_{k1} & g_{k2} & \cdots & 0 & \cdots & 0 \\ \cdots & & \cdots & & \cdots & \\ g_{n1} & g_{n2} & \cdots & 0 & \cdots & 0 \end{bmatrix} \Rightarrow \ldots$$

Step 1 Step 2

$$\ldots \Rightarrow \begin{bmatrix} g_{11} & g_{12} & \cdots & g_{1k} & \cdots & g_{1n} \\ g_{21} & g_{22} & \cdots & g_{2k} & \cdots & g_{2n} \\ \cdots & & \cdots & & \cdots & \\ g_{k1} & g_{k2} & \cdots & g_{kk} & \cdots & g_{kn} \\ \cdots & & \cdots & & \cdots & \\ g_{n1} & g_{n2} & \cdots & g_{nk} & \cdots & g_{nn} \end{bmatrix}$$

Step n

- **Step C.** *Design of the non-diagonal compensator elements* g_{ij}

  The (n-1) non-diagonal elements g_{ik} ($i \neq k$, $i = 1,2,\ldots n$) of the k-th compensator column are designed to, minimise the cross-coupling terms c_{ik} .

$$\boxed{c_{1ij} = g_{ij} - \frac{g_{jj}\left(p^*_{ij} + g_{ij}\right)}{\left(p^*_{jj} + g_{jj}\right)} = 0}$$

$$\boxed{c_{2ij} = \frac{\left(p^*_{ij} + g_{ij}\right)}{\left(p^*_{jj} + g_{jj}\right)} = 0}$$

$$\boxed{c_{3ij} = p^*_{ij} - \frac{p^*_{jj}\left(p^*_{ij} + g_{ij}\right)}{\left(p^*_{jj} + g_{jj}\right)} = 0}$$

- **Step D.** The design of the prefilter ***F*** does not present any difficulty because the final $\boldsymbol{T}_{y/r}$ function shows less loop interaction. Therefore, the prefilter ***F*** can be diagonal.

Mario Garcia-Sanz

Robust Stability of the MIMO system

- The sequential non-diagonal MIMO QFT technique introduced here arrives at a **robust stable** closed-loop system if , for each $\boldsymbol{P} \in \mathbf{TP}$,

Checked at each loop

a) each $L_i(s) = g_{ii}(s)\ (p_{ii}^{*e})^{-1}$, i=1, ..., n, satisfies the Nyquist encirclement condition,

b) no RHP pole-zero cancellations occur between $g_{ii}(s)$ and $(p_{ii}^{*e})^{-1}$, i=1, ..., n,

Checked at the end

c) no Smith-McMillan pole-zero cancellations occur between $\boldsymbol{P}(s)$ and $\boldsymbol{G}(s)$, and

d) no Smith-McMillan pole-zero cancellations occur in $|\boldsymbol{P}^*(s) + \boldsymbol{G}(s)|$

Mario Garcia-Sanz

RHP transmission zeros of the MIMO system

To remove the RHP transmission zeros that could be introduced in the previous controller design

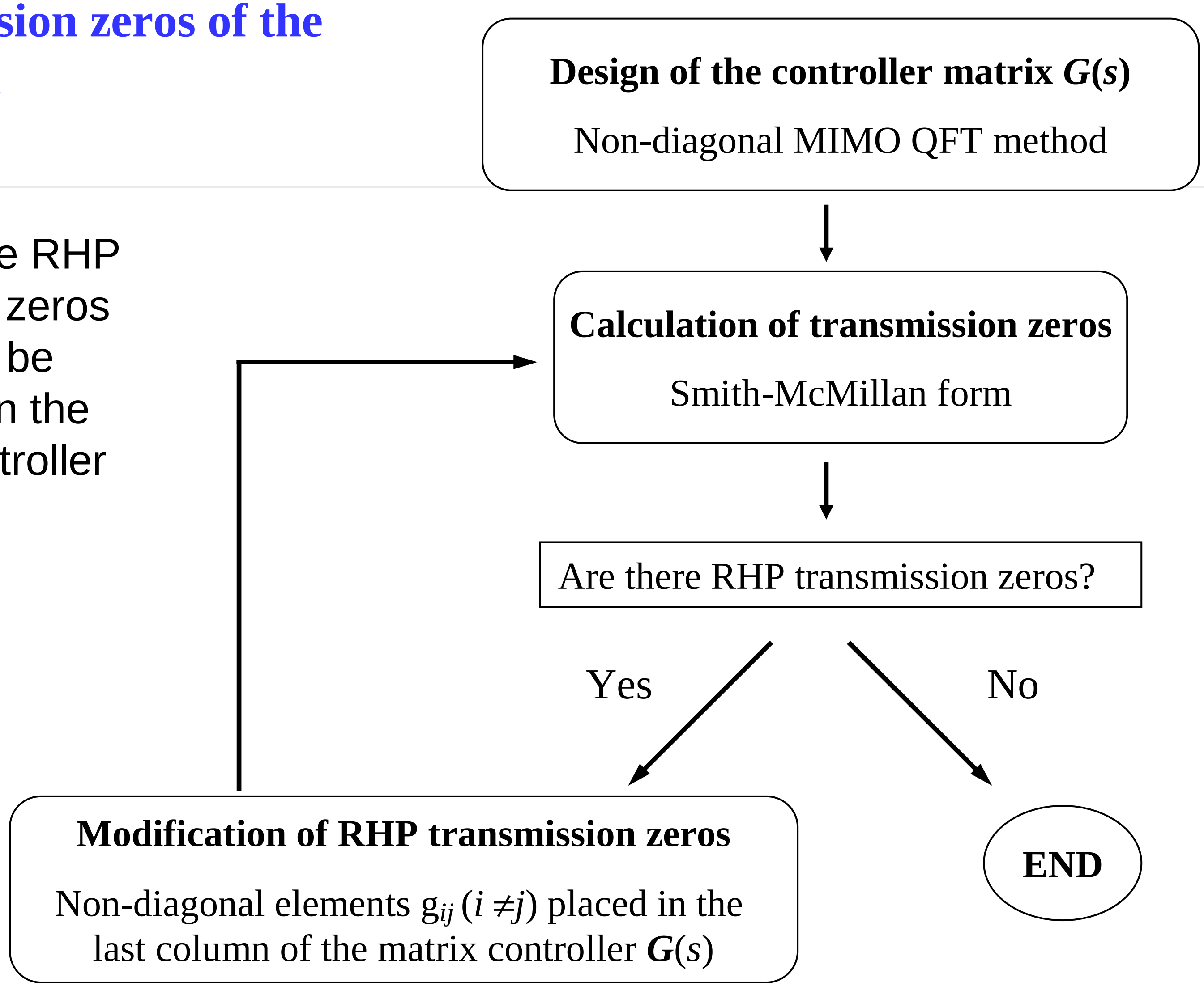

$$\begin{bmatrix} g_{11} & g_{12} & \cdots & g_{1k} & \cdots & g_{1n} \\ g_{21} & g_{22} & \cdots & g_{2k} & \cdots & g_{2n} \\ \cdots & & \cdots & & \cdots & \\ g_{k1} & g_{k2} & \cdots & g_{kk} & \cdots & g_{kn} \\ \cdots & & \cdots & & \cdots & \\ g_{n1} & g_{n2} & \cdots & g_{nk} & \cdots & g_{nn} \end{bmatrix}$$

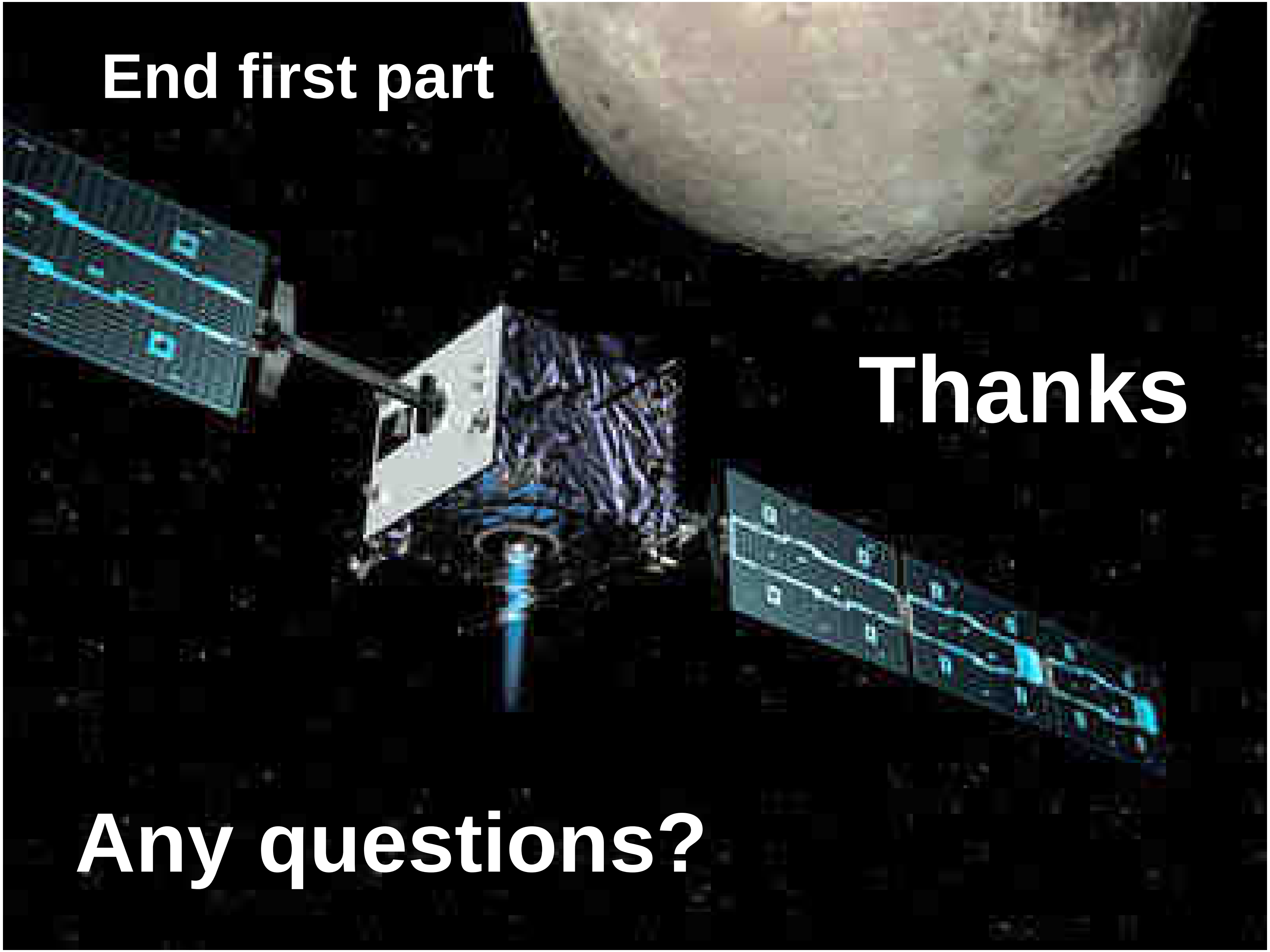
End first part
Thanks
Any questions?